Bulletin of the Mineral Research and Exploration

http://bulletin.mta.gov.tr

Petrological and geochemical features of Biga Peninsula granitoids, NW Anatolia, Turkey

Ümit AYDIN[a], Pınar ŞEN*[a], Öner ÖZMEN[a] and Erdal ŞEN[b]

[a] *General Directorate of Mineral Research and Exploration, Mineral Research and Exploration Department, 06800, Ankara, Turkey.*
[d] *Hacettepe University, Faculty of Engineering, Geological Enginerirng Department, 06532, Ankara, Turkey.*

Research Article

Keywords:
Biga Peninsula, Granitoid, Aqeous fluids, Sediment melt, Metasomatism.

ABSTRACT

In Northwest Anatolia, widespread magmatism developed due to collision between Anatolide-Tauride platform and Sakarya continent during Late Cretaceous-Early Tertiary period. The granitoids in Biga Peninsula are products of post-collisional magmatism following the convergence of the northern branch of Neotethyan Ocean and developed in two different stages as Eocene and Oligo-Miocene. Eocene Karabiga, Güreci, Kuşçayır and Dikmen granitoids are granite and diorite-granodiorite; Oligo-Miocene Sarıoluk, Yenice, Kestanbol, Eybek, Evciler, Çamyayla and Alanköy granitoids are diorite, granodiorite, monzonite and Q-monzonite in composition. Metaluminous and peraluminous granitoids have similar geochemical variations and exhibit post-collisional geochemical signatures. Trace element patterns are almost similar to those observed in upper crust and GLOSS (Global Subducting Sediment) patterns with depletion in high field strength (HFS) elements (Nb, Ta, Ti, Zr, Hf). But, Oligo-Miocene Sarıoluk, Yenice-Çakıroba, Kestanbol, Evciler, Çamyayla, Alanköy and Eocene Karabiga, Güreci and Kuşçayır granitoids have higher Th and U contents relative to upper crust and GLOSS. Dikmen, Yenice-Hamdibey, Yenice-Eskiyayla and Eybek granitoids have lower Th content. Geochemical variations indicate that partial melting and fractional crystallisation-crustal contamination processes are effective in their genesis and evolution. Trace element ratios also indicate subduction signatures in their genesis and Rb/Ba, Rb/Sr ratios suggest mantle melting rather than crustal melting. Accordingly, post-collisional Biga Peninsula granitoids were derived from a previously metasomatised lithospheric mantle source, which was enriched during northward subduction and closure of the northern branch of Neo-Tethys Ocean beneath the Sakarya continent, since variations in Rb, Cs, Th, La and Sm reveal that lithospheric mantle was mesomatised by both aqueous fluids and sediment melts.

Received Date: 26.02.2018
Accepted Date: 11.06.2018

1. Introduction

The closure of the Neo-Tethys ocean at the end of the Late Cretaceous and the following continental collision played an important role in the tectonic evolution of Anatolia. As a result of the subduction of the northern branch of the Neo-Tethys beneath the Sakarya continent to the north, continent-continent collision occurred between the Anatolide-Tauride platform and the Sakarya continent. This collision occurring along the northern section of Anatolia is represented by the İzmir-Ankara-Erzincan suture zone (IAESZ) and this suture zone separates the Sakarya zone from the Anatolide-Tauride platform (Okay and Tüysüz, 1999; Şengör and Yılmaz, 1981). The continent-continent collision is thought to have occurred before the Middle Eocene (Genç and Altunkaynak, 2007; Altunkaynak et al., 2012*a*) in the Palaeocene-Early Eocene period (Okay et al., 2001; Okay, 2008). Latest Early Eocene is accepted as the time of post-collisional extensional tectonics (Yılmaz et al., 1995; Genç and Yılmaz, 1997;

Citation Info: Aydın, Ü., Şen, P., Özmen, Ö., Şen, E. 2019. Petrological and geochemical features of Biga Peninsula granitoids, NW Anatolia, Turkey. Bulletin of the Mineral Research and Exploration, 160, 81-115. *http://dx.doi.org/10.19111/bulletinofmre. 466522*

* *Corresponding Author: Pınar ŞEN pinar.sen@mta.gov.tr*

Karacık et al., 2008). After this collision, widespread magmatic activity occurred in northwest Anatolia (Yılmaz, 1989; 1990; Güleç, 1991; Harris et al., 1994; Seyitoğlu and Scott, 1996; Altunkaynak et al., 2012*a, b*). After collision, the first products of magmatism comprised Middle Eocene-aged granitic plutons and intermediate-composition calcalkaline volcanic rocks (Harris et al., 1994; Delaloye and Bingöl, 2000; Altunkaynak and Dilek, 2006; Okay and Satır, 2006; Altunkaynak, 2007; Altunkaynak and Genç, 2008; Yılmaz Şahin et al., 2010; Altunkaynak et al., 2012*b*; Altunkaynak and Dilek, 2013; Ersoy and Palmer, 2013; Gülmez et al., 2013; Aysal, 2015; Ersoy vd., 2017*a*, *b*). It is known that the Late Oligocene-Early Miocene period magmatism produced granitic plutons and coeval volcanic rocks commonly observed in NW Turkey (Genç, 1998; Aldanmaz et al., 2000; Karacık et al., 2008; Hasözbek et al., 2010*a, b*; Yılmaz Şahin et al., 2010; Altunkaynak et al., 2012*a*; Erkül and Erkül, 2012; Aldanmaz et al., 2015; Aysal, 2015). Upper Miocene-Pliocene magmatism generally has alkaline basaltic composition (Yılmaz et al., 2001; Aldanmaz et al., 2015; Kürkcüoğlu et al., 2008).

There are two different opinions about the origin and tectonic setting of magmatism in northwest Turkey. According to the first of these, Middle Miocene magmatic rocks formed in a magmatic arc environment (Peccerillo and Taylor, 1976; Yılmaz et al., 1981; Ercan et al., 1995; Köprübaşı et al., 2000; Okay and Satır, 2006; Ustaömer et al., 2009). The second view is that these are post-collisional magmatism products and formed due to lithospheric delamination or slab break-off mechanisms (Aldanmaz et al., 2000; Köprübaşı and Aldanmaz, 2004; Dilek, 2006; Altunkaynak, 2007; Keskin et al., 2008; Kürkcüoğlu et al., 2008; Dilek and Altunkaynak, 2009; Gülmez et al., 2013). In recent years, the second view has gained more acceptance.

As the Biga Peninsula is a region where subduction, continent-continent collision and post-collisional processes may be observed, it forms a good area to research geochemical dynamics of magmatism and to reveal the effects of these processes on the genesis and the evolution of the magmatism. This study assessed the mineralogical-petrographical and geochemical features of granitic plutons located in the Biga Peninsula with the aim of determining magma source based on major oxides, trace elements and rare earth elements to explain the source properties and magmatic evolution.

2. Regional Geology

The Late Cretaceous-Early Eocene period was a tectonically active period and Tethyan evolution was effective in Western Anatolia with ophiolite emplacement, high pressure/low temperature metamorphism, subduction, arc magmatism and continent-continent collision processes occurring (Okay et al., 2001). As a result, northwest Turkey is located in an important orogenic belt where different tectonic assemblages and belts can be observed together (Şengör and Yılmaz, 1981; Okay, 1989; Okay et al., 1996; Okay and Tüysüz, 1999; Okay et al., 2001). These tectonic assemblages are separated from each other by sutures represented by ophiolites, metamorphic rocks and accretionary complexes (Okay et al., 2001). The Biga Peninsula comprises two different tectonic assemblages separated from each other by the Intra-Pontide Suture Zone in the northwest; these assemblages are the Rhodope-Istranca massif to the north and the Sakarya assemblage to the south (Figure 1a). The Sakarya assemblage is bounded by the Intra-Pontide suture zone to the north and the İzmir-Ankara-Erzincan suture zone to the south (Figure 1a). The basement of the assemblage is Palaeozoic-aged metamorphic and plutonic rocks (Okay et al., 1996; Delaloye and Bingöl, 2000; Okay et al., 2006; Topuz et al., 2007; Okay, 2008) and the Permo-Triassic-aged (subduction/addition complex) accretionary complex known as the Karakaya complex which underwent severe deformation and partial metamorphism (Okay et al., 1996; Okay and Göncüoğlu, 2004; Okay et al., 2006; Okay, 2008). The complex basement is unconformably overlain by Lower-Middle Jurassic continental-shallow marine clastic sedimentary rocks (Altıner et al., 1991; Okay, 2008) and Middle-Upper Jurassic platform-type neritic limestones, Lower Cretaceous limestones and Upper Cretaceous-Palaeocene volcanic and sedimentary rocks (Akyüz and Okay, 1996; Okay et al., 1996; Okay and Tüysüz, 1999; Okay, 2008).

The Biga Peninsula has complicated geology comprising variable metamorphic, magmatic and sedimentary rocks with ages from the Palaeozoic to the Cenozoic. Since the main subject of this study comprises the mineralogical-petrographical and geochemical features of Eocene and Oligo-Miocene-aged granitoids in the Biga Peninsula, the geology of the region has been simplified (Figure 1). Rocks outcropping in the Biga Peninsula may be divided in

two as pre-Tertiary basement rocks and Tertiary rocks (Duru et al., 2012). In the study area, pre-Tertiary basement rocks outcrop within NE-SW striking tectonic zones (Duru et al., 2012). These zones are the Çetmi melange, Ezine zone and Sakarya Zone from west to east (Figure 1b).

The Sakarya Zone forming the basement in the study area comprises the underlying Kazdağ metamorphics and tectonically associated Kalabak Group and Karakaya complex. All these units are unconformably overlain by Jurassic-Cretaceous-aged neritic carbonates (Figure 1b). Ezine Zone which is outcropped in the NW of the peninsula, is represented by the Karadağ Group, Çamlıca metamorphics and the Denizgören ophiolite overlying these units with a tectonic contact. The Ezine and Sakarya zones are overlain by the Upper Cretaceous-aged Çetmi Melange (Duru et al., 2012) (Figure 1b).

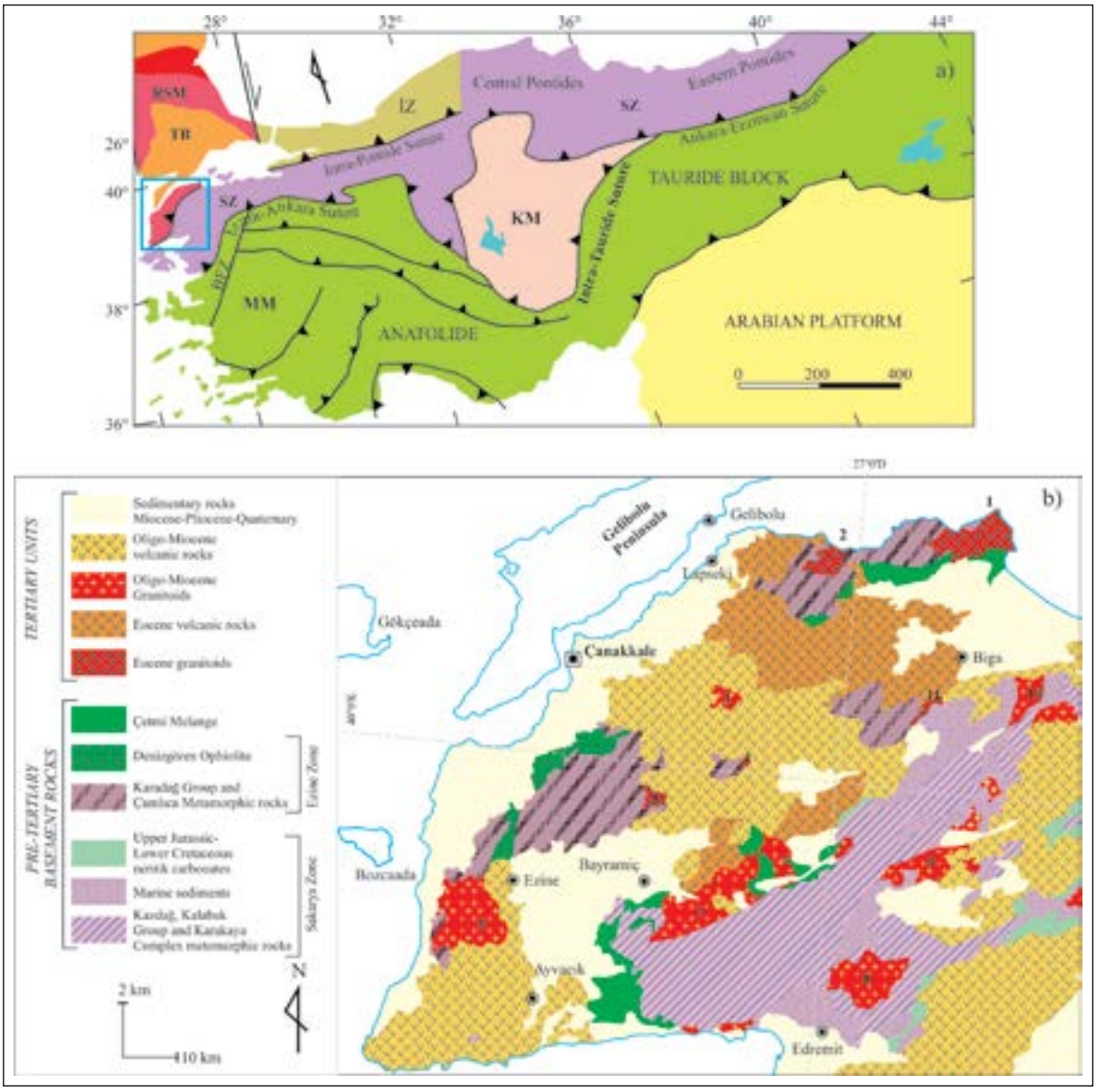

Figure 1- a) Tectonics of Turkey (Okay and Tüysüz, 1999). RSM: Rhodope-Strandja Massif; TB: Thace basin; İZ: İstanbul Zone; SZ: Sakarya Zone; MM: Menderes Massif; KM: Kırşehir Massif; BFZ: Bornova Flysch Zone. b) Generalised geological map of Biga Peninsula (Konak et al., 2016; Duru et al., 2012; Ersoy et al., 2017*a, b*). *1*: Karabiga pluton; *2*: Güreci pluton; *3:* Çamyayla pluton; *4*: Alanköy pluton; *5:* Kuşçayır pluton; *6*: Kestanbol pluton; *7*: Evciler pluton; *8*: Eybek pluton; *9*: Yenice pluton; *10*: Sarıoluk pluton; *11*: Dikmen pluton.

Above these pre-Tertiary basement rocks in the study region, magmatic and sedimentary rocks occurred during the Eocene-Quaternary time interval were emplaced (Duru et al., 2012; Ilgar et al., 2012). In the Biga Peninsula, Tertiary plutonic and volcanic rock units are widespread throughout the region. The Tertiary period begins with Eocene granitoids and andesitic-dacitic calcalkaline volcanic rocks and continues in the Upper Miocene with alkaline character basaltic volcanic rocks (Yılmaz, 1990).

Magmatism developing as a result of collision between the Sakarya continent and Anatolide-Tauride platform in the Late Cretaceous-Early Tertiary period produced its first products in the Middle Eocene and continued until the end of the Miocene (Yılmaz, 1997; Karacık and Yılmaz, 1998; Genç and Altunkaynak, 2007; Yılmaz Şahin et al., 2010). The granitoids forming the subject of the study and outcropping over large areas were emplaced in the region in the Eocene and Oligocene-Miocene time interval. The age of the granitoid rocks in the Biga Peninsula becomes younger from Middle Eocene in the north to Oligo-Miocene in the south. This study focuses on the mineralogical, petrographical and geochemical features of the Eocene granitoid rocks of the Karabiga and Güreci granitoids outcropping east of Lapseki and around Karabiga in the north of the Biga Peninsula, Kuşçayır granitoid to the north of Bayramiç, Dikmen granitoids to the south of Biga and the Oligo-Miocene Eybek, Evciler, Kestanbol, Çamyayla, Alanköy, Sarıoluk and Yenice granitoids generally outcropping in the south of the peninsula.

Karabiga granitoid is located north of Karabiga, covering nearly 75 km^2 area and generally has granitic composition. There are many dikes (pegmatite and aplite dikes) extending in different directions within the pluton. Aplite dikes are elongated mainly N-S direction, with a thickness up to 1.5 m. Pegmatite dikes are generally extending in N60-80°W direction. The basement rocks in the area of the Karabiga granitoid comprises lithologic units such as mica schist, amphibolite schist and gneiss belonging to Permo-Triassic-aged Çamlıca metamorphic rocks. The Upper Cretaceous Çetmi ophiolite tectonically overlies this unit (Duru et al., 2012) and the Karabiga granitoid has been emplaced by cutting both these units.

Güreci granitoid outcropping over 22 km^2 area around the Çavuşköy and Güreci were first called the Şevketiye granitoid by Delaloye and Bingöl (2000). They are petrographically classified as granodiorite, monzonite and quartz diorite. The Güreci granitoid has experienced intense alteration, fresh outcrops are found only in some stream beds. There are dioritic mafic enclaves hosted within the rock.

Kuşçayır granitoid is mostly represented by dark colored diorite, diorite-porhyry and light colored granodiorite type rocks and it is white, gray and yellowish in color due to weathering. Contact metamorphic zone representing the hornblende hornfels and albite-epidote hornfels facies is developed along the contact with host rock. Plutonic rocks, cutting quartzite and mica-schist, are overlain by volcanic rocks at the ENE of Kuşçayır village.

Dikmen granitoid with a NE-SW trending in the east of Dikmen fault has coarse grained crystals and is greyish white in color. They are usually cut by quartz veins/veinlets which have up to 50 cm. thickness and aplites. The number of quartz veins/veinlets increase from north to south.

Sarıoluk granitoid is located west of Gönen County between Balıkesir and Çanakkale provinces. The unit is brownish-greenish colour, highly weathered, with abundant biotite flakes, metagranite with clear foliation and gneissic granite appearance and petrographically granodiorite composition. Pegmatite veins containing abundant quartz and alkali feldspar are observed cutting the base of the unit in the study area. The unit has tectonic contacts with all surrounding units.

Yenice granitoids, which are usually light colored, are mostly represented by monzonitic and granodioritic rocks, and generally extending in NE-SW direction in the vicinity of Yenice, Hamdibey, Eskiyayla and Çakıroba. Contact metamorphism developed at the contact of plutons. They are abundantly cracked and articulated, and often cut by aplite dykes.

Kestanbol granitoid is grey-brown in colour, with occasional K-feldspar of 4-5 cm cut by lamprophyre in the study area that typically outcrops around Kestanbol and Koçali village. The Kestanbol granitoid is lithologically homogeneous comprising quartz monzonite, monzonite, monzonite porphyry and granite rock types. Aplite, lamprophyre and mafic dikes were emplaced into the fractuıre planes in the Kestanbol granitoid. The pluton was emplaced within metamorphic basement rocks and there is a

contact metamorphic zone and skarn mineralization at the contact with basement rocks. There are many lamprophyre dikes within the pluton.

Eybek granitoid is a pluton represented by granite, Q-monzonite and granodiorite rocks with N-S, NW and NE trending veins in the east section. Some sections of the pluton are weathered and rounded forms with 30-50 cm diameter are observed due to weathering. Additionally, mafic enclaves are enclosed.

Evciler granitoid is an elliptical body covering nearly 180 km^2 area with WSW-ENE trending. Topography in the area of outcrops is smooth. It was emplaced into the basement rocks and lower volcanic units. An albite-epidote-hornfels facies zone reaching up to 200 m width developed on the contact with Kazdağ metamorphic rocks. Mafic enclaves of various size are observed.

Çamyayla granitoid outcrops around Çan and is coeval with the adjacent Dededağ volcanic assemblage. Products developing during this process are defined by both cross-cutting and overlapping associations. A contact metamorphic zone with actinolite hornfels and quartz-alkali feldspar hornfels facies developed around the pluton.

Alanköy granitoid represented by granodioritic rocks has well developed skarn zones and Q-stockworks as well.

3. Petrographic Features of Biga Peninsula Granitoids

The granitoids in the study area are mostly classified as granite and granodiorite (Appendix 1). In addition, the Güreci, Kestanbol, Kuşçayır, Alanköy and Çamyayla granitoids are called as monzonite, Q-monzonite, Q-monzodiorite and Q-diorite rock types. The granitoids in the region occur as widespread plutonic bodies, and aplite and porphyry dikes having mineralogical composition similar to granitoids occurred as planar intrusions are observed as well. The majority of this type of dikes are observed in the Karabiga, Kestanbol and the Çamyayla granitoids. Almost all samples have holocrystalline texture. Most of the samples having moderate-large grain size exhibit granular texture, whereas dikes have fine-moderate grain size and porphyric texture. The main mineral phases are quartz, plagioclase, orthoclase, hornblende and biotite, with relatively lesser amounts of microcline and clinopyroxene minerals (Figure 2). Titanite, apatite and opaque minerals are common accessory minerals. Secondary chlorite, sericite, calcite and clay minerals are observed in almost all rocks due to alteration.

Quartz is generally anhedral and crystallised as space-fillings between other minerals. Typically it has undulatory extinction. It is subhedral in Karabiga aplitic rocks and significant reduction is observed in grain size.

Plagioclase is the main component of the granitoids. Many plagioclase minerals have polysynthetic twinning in addition to zoned texture. Generally, there is little or partial sericitisation. Especially in the Evciler granitoids, common myrmekitic texture is observed along grain boundaries. In the Yenice-Eskiyayla granitoids, sieve texture is observed due to excessive alteration. The alteration effect is very limited in the Sarıoluk granitoids.

Alkali feldspar is mainly observed as orthoclase minerals. Microcline is only observed in the Yenice-Eskiyayla granitoids. In all samples, orthoclase generally found as large crystals, has experienced alteration, and more argillized or sericitized than plagioclase minerals. Due to large grain size, they have poikilitic texture enclosing quartz and hornblende minerals especially in the Güreci, Eybek, Kestanbol and Evciler granitoids. In the Karabiga, Yenice-Eskiyayla, Çamyayla, Alanköy and Sarıoluk granitoids, perthitic texture, graphic texture and rare granophyric texture developed.

Hornblende is generally found as long prismatic crystals. They are less common in the Karabiga and Kestanbol granitoids than in other regions. Some of the hornblendes in the Evciler, Yenice-Çakıroba and Sarıoluk granitoids formed from the edges and the cleavages of the pyroxene. As the transformation of pyroxene to amphibole is not complete, pyroxene residues remain. This situation may be explained by rapid volatile loss from granitic magmas (Poutiainena and Scherbakovab, 1998). In some samples, and especially in the Dikmen and Yenice-Hamdibey region, poikilitic texture containing plagioclase minerals has developed. Exsolution of opaque from the cleavage is noteworthy in Eybek and Kuşçayır granitoids. Hornblende in the Çamyayla, Alanköy

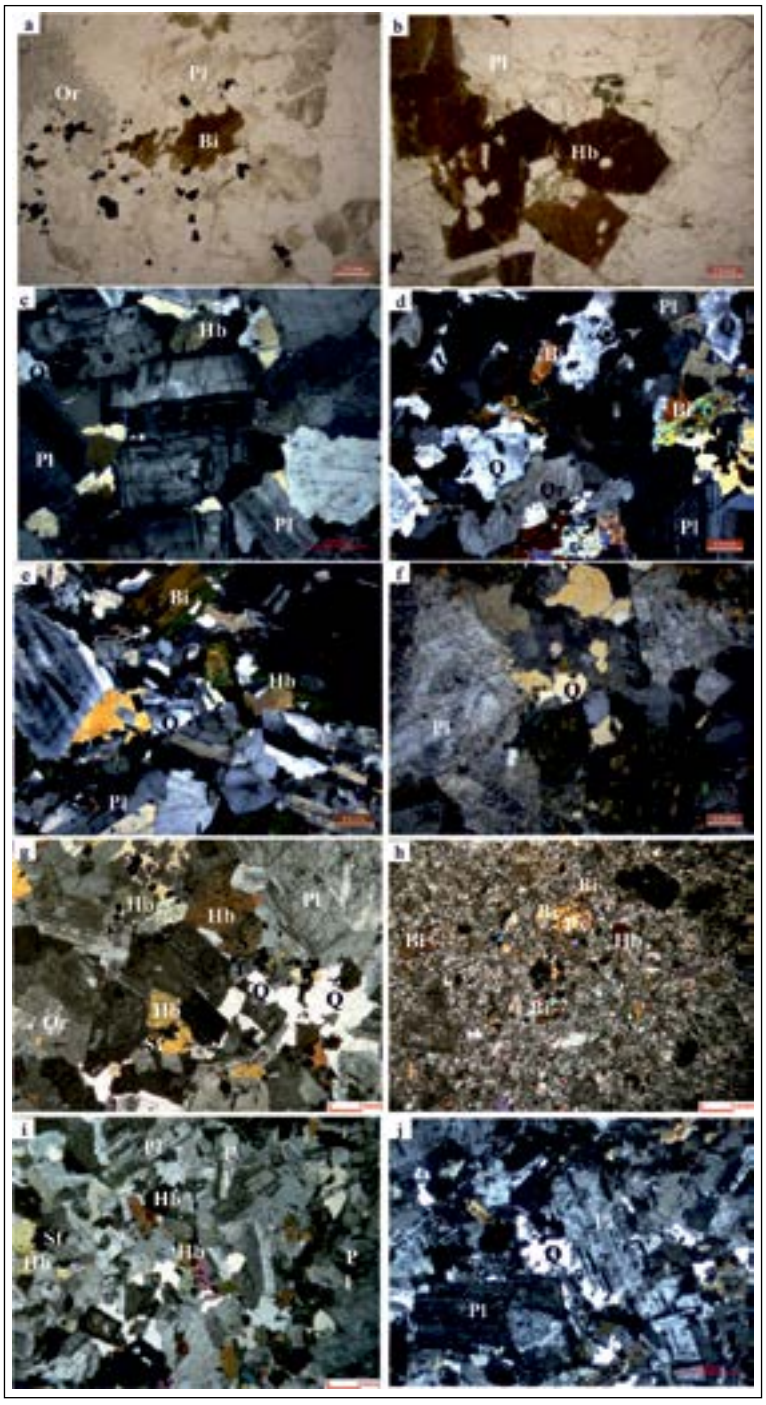

Figure 2- Microphotographs from Biga Peninsula granitoids; a) Granite with a granular texture from Karabiga (plane polarised x 2.5); b) Granite with a granular texture from Güreci granitoid (plane polarised x 2.5); c) Granodiorite with a granular texture from Dikmen granitoid (cross polarised x 2.5); d) Granodiorite sample from Sarıoluk (cross polarised x 2.5); e) Granodiorite from Evciler granitoid (cross polarised x 2.5); f) Q-diyorit sample from Alanköy granitoid (cross polarised x 2.5); g) Q-monzonite sample from Kestanbol granitoid (cross polarised x 2.5); h) Porphyric lamprophyr sample from Kestanbol granitoid (cross polarised x 2.5); i) Monzonite with a holocrystalline granular texture from Kestanbol granitoid (cross polarised x 2.5); j) Q-monzodiorite with a holocrystalline porphyric texture from Kuşçayırı granitoid (cross polarised x 2.5). Bi: biotite; Hb: hornblende; Or: orthoclase; Pl: plagioclase; Px: pyroxene; Q: Quartz; Sf: sphene (titanite).

and Sarıoluk granitoids have been carbonatised and in some parts they are altered to chlorite.

Clinopyroxene minerals have not remained stable, and largely transformed to hornblende minerals. In some samples (Sarıoluk granitoid), though they retain their original crystal form, they are generally observed as residues in the hornblende minerals.

Biotite is found less than hornblende but is the dominant dark-coloured mineral in the Karabiga granitoid, especially, and in dikes in other regions. Generally, they have been chloritised by alteration in the Yenice-Çakıroba, Hamdibey and Evciler granitoids.

Titanite is euhedral crystals in nearly all rocks. Apatite which is rarely observed in the samples, is found as needle-like and prismatic crystals, and it mainly occur as inclusions.

4. Analytical Techniques

Major oxides, trace and rare earth element analyses were performed in General Directorate of Mineral Research and Exploration (MTA), Mineral Analysis and Technology Department. Major oxide analyses were performed by using a Thermo ARL XRF device with 3 g samples mixed with cellulose binder (0.9 g), pressed into pellet form at 40 kN pressure.

Trace and rare earth element analyses were performed by Plasma Quant MS Elite Analytic Jena ICP-MS device. Samples of 0.25 g were dissolved in HCl, HNO_3, $HClO_4$ and HF acids and the dissolved sample was completed to 50 ml for analysis. JG 1a Certified Reference Material was used for quality control of the analysis. The values measured during analysis of certified standard reference material are given in table 1.

5. Geochemical Features of Biga Peninsula Granitoids

The major oxide, trace and rare earth element analysis for granitoids in the Biga Peninsula are given in Table 1. To classify the rocks, the major oxides were normalised to 100% on an anhydrous basis and plotted on a total alkali (Na_2O+K_2O %) - SiO_2% diagram (Figure 3). According to Middlemost (1994)'s volcanic rock classification diagram, Eocene Karabiga, Güreci, Kuşçayır and Dikmen granitoids in Biga Peninsula are granite, diorite and granodiorite in composition, respectively and Oligo-Miocene granitoids are diorite, granodiorite, monzonite and Q-monzonite in composition. They all exhibit subalkaline major-oxide character (Figure 3). Subalkaline rocks exhibit calcalkaline signature according to the AFM diagram with calcalkaline-tholeiitic dividing line (Irvine and Baragar, 1971) (Figure 3).

Variation diagrams for major oxides and some selected trace elements against SiO_2 (Harker diagrams) are shown in figure 4. Increasing SiO_2 is correlated with (i) decreasing Fe_2O_3, MgO, CaO, Al_2O_3, Sr and Nb and (ii) increasing K_2O and Rb. These observed variations in Fe_2O_3, MgO, CaO, Al_2O_3, Sr, and the relative increase in K_2O and Rb with increasing SiO_2 may indicate fractional crystallisation processes. Na_2O exhibits a relatively horizontal trend with increasing SiO_2. This situation may be due to weathering. It can be concluded that fractional crystallisation processes played a role in the evolution of Biga granitoids.

In the plot of Shand (1943)'s A/NK – A/CNK diagram (Figure 5a), Karabiga samples are generally metaluminous, samples from other granitoids are metaluminous to peraluminous. Most of the samples clearly plot in the I-type granite field. On the ASI-Fe_{tot} diagram of Norman et al. (1992), the majority of samples also represent I-type granite features (Figure 5b). As a result, the Biga Peninsula granitoids exhibit both metaluminous and peraluminous composition. They have MgO/MnO and MgO/Fe_2O_{3t} ratios generally varying from 3 to 27 and 0.20 to 0.52, respectively and Na_2O/CaO ($\leq$4.86) and A/NK (>1.2) values, reflecting the characteristics of continental arc granites (Maniar and Piccoli, 1989).

Primitive mantle (Sun and McDonough, 1989) normalised trace element distribution diagrams of Biga Peninsula granitoids are shown in figure 6. As can be seen on the diagrams, the common features to all the granitoids in the Biga Peninsula are the depletion in Nb, Ta, Zr and Ti elements and the enrichment in Pb and U elements. These observed variations are common geochemical features of arc magmatism and also may form as a result of contamination by continental crust during the upwelling of mantle-derived magmas. Accordingly, negative anomalies in Nb, Ta and Ti and positive anomalies in Pb and U are the most typical features of crustal contamination and/or sediment contribution to mantle-derived

Table 1- Major-oxide (wt.%), trace and rare earth elements (ppm) analysis of Biga Peninsula granitoids (wt. %: weight %; LOI: Loss on ignition)

	KARABİGA GT						GÜRECİ GT							
Sample No	ASM-K11	ASM-K12	ASM-K13	ASM-K14	ASM-K15	ASM-K16	ASM-K01	ASM-K02	ASM-K03	ASM-K04	ASM-K05	ASM-K06	ASM-K07	ASM-K08
SiO_2 (wt.%)	76.1	73.9	73.9	74	72.5	75.4	65.1	64.6	66.1	67.2	62.8	54.2	60.2	59
TiO_2	0.1	0.2	0.2	0.2	0.2	0.1	0.5	0.5	0.5	0.4	0.5	0.5	0.6	0.7
Al_2O_3	13.2	14	13.7	14	15.1	13.6	16.4	16.3	16.2	16.2	16.8	20	17.4	18.3
CaO	0.4	1.6	1.7	1.5	2.1	2.4	4.8	2.2	4.4	3.8	5.9	7.6	5.9	7.7
Fe_2O_3t	1	1.5	1.5	1.5	1.5	0.9	4.6	5.3	4.2	3.5	5.1	8	5.9	4.6
Na_2O	3.1	3.4	3.2	3.4	3.8	3.3	3.2	3.2	3.3	3.2	2.9	4.9	3	3.9
K_2O	5.2	4	4.9	4.4	3.7	3.2	2.6	3.6	2.8	3.2	2.8	1	2.9	1.8
MgO	0.1	0.3	0.3	0.3	0.3	0.3	1.6	1.8	1.5	1.1	1.9	2.3	2.2	2.4
MnO		0.1					0.1	0.2	0.1	0.1	0.1	0.1	0.1	0.1
P_2O_5		0.1	0.1	0.1	0.1	0.1	0.2	0.2	0.2	0.1	0.2	0.3	0.3	0.3
LOI	0.45	0.45	0.35	0.35	0.5	0.35	0.7	1.9	0.6	0.8	0.7	0.8	1.1	1
Total	99.65	99.55	99.85	99.75	99.8	99.65	99.8	99.8	99.9	99.6	99.7	99.7	99.6	99.8
A/CNK	1.15	1.09	1.00	1.07	1.07	1.02	0.97	1.24	0.98	1.03	0.91	0.87	0.92	0.82
A/NK	1.23	1.41	1.29	1.35	1.47	1.53	2.03	1.78	1.91	1.85	2.15	2.19	2.15	2.19
Sc (ppm)	13	14	2	2	2	2	14	13	10	9	12	27	4	12
V	31	21	25	24	26	19	101	112	105	93	132	218	151	166
Cr	163	211	124	220	195	190	155	141	184	173	148	40	93	68
Rb	211	146	166	144	125	75	76	112	94	98	78	34	96	67
Sr	48	116	96	93	136	228	249	229	284	273	351	579	515	544
Y	17	18	12	10	14	13	23	20	16	15	15	97	7	15
Zr	45	24	21	32	17	11	13	12	11	10	14	11	10	13
Nb	17	14	12	14	11	11	10	11	11	11	8	23	8	9
Cs	4	4	5	4	5	1	2	2	3	4	3	2	3	3
Ba	73	330	218	229	248	679	483	748	624	772	733	104	753	254
La	33	31	28	30	29	33	36	27	32	22	23	30	10	22
Ce	61	58	49	47	52	56	66	52	56	44	43	72	21	43
Pr	6	6	4	4	5	5	6	5	5	4	4	8	2	4
Nd	22	22	14	14	14	15	20	17	16	16	15	38	7	15
Sm	4	4	2	2	2	3	4	3	3	3	3	12	1	3
Eu	1.06	1.22	0.25	0.47	0.54	0.47	1.01	0.92	0.8	0.91	0.87	2.27	0.44	0.82
Gd	3.2	3.6	2.2	2.2	2.3	2.4	3	2.7	2.4	2.3	2.4	9.6	1.1	2.3
Tb	0.54	0.56	0.34	0.31	0.35	0.35	0.57	0.52	0.43	0.41	0.45	2.39	0.2	0.42
Dy	3.1	3.1	2	1.7	2.2	2	3.5	3.2	2.5	2.5	2.6	15.9	1.2	2.5
Ho	0.58	0.59	0.4	0.34	0.42	0.4	0.68	0.62	0.49	0.46	0.51	3.07	0.22	0.49
Er	1.96	2	1.55	1.23	1.58	1.45	2.33	2.11	1.67	1.55	1.68	10.34	0.75	1.63
Tm	0.2	0.2	0.2	0.2	0.2	0.2	0.3	0.3	0.2	0.2	0.2	1.4	0.1	0.2
Yb	1.7	1.7	1.9	1.3	1.8	1.6	2.1	1.9	1.5	1.4	1.5	9.2	0.7	1.5
Lu	0.26	0.25	0.31	0.2	0.29	0.25	0.32	0.3	0.23	0.22	0.24	1.3	0.1	0.22
Hf	3.2	1.6	1.3	1.8	1.0	0.8	1.3	1.2	1.1	0.9	1.4	1.7	1.0	1.3
Ta	1.9	1.3	1.2	1.1	1.0	0.6	0.8	0.8	0.7	0.8	0.7	1.8	0.5	0.6
Pb	37	776	25	24	20	22	17	252	20	18	16	13	16	14
Th	77	61	132	76	96	97	95	72	73	74	63	92	37	64
U	18	18	18	19	18	18	21	18	16	17	17	22	9	17

Table 1- (Continued)

			KUŞÇAYIR GT					DİKMEN GT			SARIOLUK GT			
Sample No	ASM-K09	ASM-K10	ASM-K48	ASM-K49	ASM-K50	ASM-K51	ASM-K52	ASM-K56	ASM-K57	ASM-K58	ASM-K25	ASM-K26	ASM-K27	ASM-K28
SiO_2 (wt.%)	60.8	61.6	61.4	61.2	61.2	61.7	56.7	66.2	65.6	64.5	64	64	64	66.2
TiO_2	0.5	0.6	0.5	0.6	0.5	0.6	0.7	0.3	0.3	0.4	0.6	0.5	0.6	0.5
Al_2O_3	17.4	17.2	17	17.3	17.3	16.8	17.6	17.6	18.2	18.7	16.4	16.3	16.2	15.8
CaO	5.7	6	6	5.7	6.3	5.9	6.8	4.5	4.9	4.5	4.4	4.3	4.5	3.8
Fe_2O_3t	5.6	5.5	5.2	5.5	5.3	5.5	7	2.8	2.6	2.7	4.3	4.4	4.4	3.8
Na_2O	3.1	3.1	3.1	3	3.2	3.1	2.9	4.5	4.9	4.6	3.5	3.5	3.4	3.3
K_2O	2.8	2.8	2.9	2.7	2.6	2.8	2	1.8	1.3	1.5	3.9	3.8	3.8	3.9
MgO	2.1	2	2.1	2.2	2.1	2.1	3	1.2	1.1	1.4	1.7	1.7	1.8	1.5
MnO	0.1	0.1	0.1	0.2	0.1	0.1	0.2	0.1	0.1	0.1	0.1	0.1	0.1	0.1
P_2O_5	0.3	0.2	0.2	0.3	0.3	0.3	0.3	0.2	0.1	0.2	0.3	0.3	0.3	0.2
LOI	1.15	0.65	1.15	1.2	0.8	0.95	2.55	0.6	0.6	1.15	0.45	0.65	0.55	0.55
Total	99.55	99.75	99.65	99.9	99.7	99.85	99.75	99.8	99.7	99.75	99.65	99.55	99.65	99.65
A/CNK	0.94	0.90	0.89	0.95	0.88	0.89	0.91	1.00	0.99	1.08	0.91	0.92	0.90	0.95
A/NK	2.14	2.11	2.06	2.20	2.14	2.06	2.54	1.88	1.92	2.03	1.64	1.65	1.67	1.64
Sc (ppm)	15	18	12	10	14	19	23	7	6	8	2	2	10	9
V	151	141	147	149	140	4	4	3	3	4	120	117	122	108
Cr	97	117	87	92	80	21	8	35	25	35	119	127	131	163
Rb	94	88	98	44	54	116	61	63	36	62	161	146	160	157
Sr	489	517	528	514	541	951	974	841	728	988	572	543	584	511
Y	16	21	16	12	25	22	20	15	9	12	11	9	13	13
Zr	9	11	13	18	12	23	100	4	4	5	5	6	7	6
Nb	8	8	10	10	9	11	50	2	2	2	17	15	16	14
Cs	3	4	4	2	3	3	2	9.5	1	1	10	8	8	8
Ba	594	711	681	707	751	844	642	481	352	462	1155	1112	1235	1138
La	30	32	32	38	37	38	27	24	21	15	27	27	26	21
Ce	58	62	67	73	76	68	51	44	37	28	47	45	47	41
Pr	5	6	7	7	8	7	6	5	4	3	4	4	4	4
Nd	21	24	28	26	33	29	25	19	14	13	14	13	17	15
Sm	4	5	5	4	6	5.5	5	3.3	2.4	2.6	2	2	3	3
Eu	1.16	1.37	1.62	1.35	1.52	1.6	1.5	1	0.8	1	0.43	0.55	1.03	0.88
Gd	3.1	3.8	5.9	5.2	7.4	5.1	4.8	3.5	2.6	2.6	2.4	2.4	3.2	2.8
Tb	0.51	0.67	0.67	0.55	0.94	0.8	0.7	0.5	0.3	0.4	0.33	0.3	0.44	0.42
Dy	2.8	3.9	3.1	2.5	4.8	4.2	3.8	2.7	1.8	2.2	1.9	1.6	2.4	2.4
Ho	0.53	0.73	0.57	0.45	0.92	0.7	0.6	0.4	0.3	0.4	0.35	0.31	0.47	0.46
Er	1.75	2.42	2.11	1.67	3.34	2.2	2.1	1.5	1	1.3	1.32	1.16	1.66	1.62
Tm	0.2	0.3	0.3	0.2	0.4	0.4	0.3	0.2	0.2	0.2	0.2	0.2	0.2	0.2
Yb	1.5	2	1.9	1.5	2.9	2.5	2.2	1.6	1	1.3	1.5	1.3	1.5	1.5
Lu	0.21	0.29	0.26	0.21	0.39	0.4	0.4	0.3	0.2	0.3	0.23	0.19	0.22	0.22
Hf	1.1	1.2	1.0	1.4	1.0	1.6	2.8	0.4	0.3	0.4	0.5	0.7	0.9	0.7
Ta	0.6	0.6	0.5	0.5	0.5	1	0.6	0.7	0.4	0.6	1.2	1.0	1.0	1.0
Pb	18	20	73	36	18	43	29	12	10	9	89	41	43	67
Th	63	55	96	107	92	0.9	0.6	0.3	0.2	0.2	86	77	70	73
U	17	18	26	22	24	4.8	3.1	1.1	0.7	1	19	20	21	20

Table 1- (Continued)

			YENİCE GT										
			Çakıroba	Çakıroba	Çakıroba	Hamdibey	Hamdibey	Hamdibey	Hamdibey	Hamdibey	Eskiyayla	Eskiyayla	Eskiyayla
Sample No	ASM-K29	ASM-K30	ASM-K31	ASM-K32	ASM-K33	ASM-K59	ASM-K60	ASM-K61	ASM-K62	ASM-K63	ASM-K53	ASM-K54	ASM-K55
SiO_2 (wt.%)	63.9	63.1	63.7	61.2	63	63.1	64.5	63.1	62.3	62.2	69.7	67.8	65.3
TiO_2	0.6	0.6	0.6	0.6	0.6	0.6	0.5	0.7	0.6	0.7	0.3	0.3	0.4
Al_2O_3	15.9	16	16.2	16	16.3	16	15.9	15.5	16.1	16.1	15.7	15.8	15.9
CaO	4.8	5	4.5	4.9	5.1	4.7	4.3	5	5.1	5.2	1.3	2.8	4.5
Fe_2O_3t	4.3	4.5	4.7	4.6	4.9	4.8	4.5	5	5.2	5.2	2.8	3.3	3.7
Na_2O	3.1	3.2	3.2	3.2	3.3	3.4	3.2	2.8	3.2	3.3	4.3	3.9	3.7
K_2O	4.2	4.1	3.8	3.9	3.5	3.7	4	4.5	3.8	3.6	3.2	3	2.3
MgO	1.9	2	2	2.2	2	2	1.8	2.1	2.1	2.2	0.8	1.3	1.5
MnO	0.1	0.1	0.1	0.1	0.1	0.1	0.1	0.1	0.1	0.1	0.1	0.1	0.1
P_2O_5	0.3	0.3	0.3	0.3	0.3	0.3	0.3	0.3	0.3	0.3	0.1	0.1	0.2
LOI	0.6	0.7	0.6	2.7	0.65	0.95	0.5	0.45	0.8	0.75	1.35	1.4	2.05
Total	99.7	99.6	99.7	99.7	99.75	99.65	99.6	99.55	99.6	99.65	99.65	99.8	99.65
A/CNK	0.86	0.85	0.92	0.87	0.88	0.88	0.91	0.83	0.86	0.86	1.22	1.07	0.95
A/NK	1.65	1.65	1.73	1.68	1.77	1.67	1.66	1.63	1.71	1.72	1.49	1.63	1.85
Sc (ppm)	17	14	12	13	13	16	12	13	17	17	5	8	7
V	114	114	122	117	125	4	4	4	5	4	3	3	3
Cr	54	60	132	128	117	26	26	13	28	23	32	27	26
Rb	156	151	151	162	130	188	164	166	189	165	97	101	53
Sr	587	579	546	506	564	1184	806	800	1150	1048	439	686	653
Y	32	22	23	23	22	24	21	26	24	28	11	23	18
Zr	7	7	7	5	7	12	10	10	12	11	7	10	7
Nb	18	16	15	15	14	6	5	5	6	6	4	5	3
Cs	10	8	8	12	6	5	5	7	7	8	2	1	1
Ba	1239	1197	1030	1107	1201	1591	1014	888	1432	1261	773	1141	948
La	54	88	42	40	39	67	44	51	66	65	40	38	31
Ce	117	163	86	80	80	123	92	93	121	126	70	64	55
Pr	12	17	9	8	8	13	11	11	13	14	7	7	6
Nd	45	66	34	31	32	52	42	44	53	57	26	27	23
Sm	8	11	6	6	6	8.7	7.2	8.1	9.2	10	4.2	4.7	4.1
Eu	1.99	2.46	1.45	1.37	1.33	2.3	1.6	1.7	2.3	2.3	1.1	1.4	1.3
Gd	8.3	10.9	6.3	6	6.1	8.8	7.3	7.9	9.3	10	3.9	4.7	4.2
Tb	1.12	1.17	0.83	0.78	0.82	1	0.9	1	1.1	1.2	0.5	0.7	0.6
Dy	5.9	4.8	4.4	4.1	4.2	4.9	4.2	5.3	5.2	5.9	2.2	3.9	3.2
Ho	1.09	0.79	0.81	0.78	0.81	0.8	0.7	0.8	0.8	0.9	0.3	0.7	0.5
Er	3.86	2.77	2.85	2.74	2.82	2.6	2.3	2.9	2.8	3.2	1.3	2.4	1.9
Tm	0.5	0.3	0.4	0.3	0.3	0.4	0.3	0.4	0.4	0.5	0.2	0.4	0.3
Yb	3.4	2	2.5	2.4	2.4	2.6	2.3	2.9	2.7	3.1	1.3	2.6	2
Lu	0.48	0.27	0.35	0.34	0.34	0.5	0.5	0.5	0.5	0.6	0.3	0.5	0.4
Hf	0.8	0.7	1.0	0.5	0.9	0.9	0.8	0.8	0.9	1	0.5	0.7	0.5
Ta	1.5	0.9	1.0	1.1	0.9	1.6	1.4	1.7	1.5	2.1	0.7	0.8	0.6
Pb	47	42	33	30	32	35	27	44	47	42	18	21	18
Th	110	182	97	92	89	2.3	2.1	2.3	2.3	2.6	1.1	1.1	0.8
U	23	33	22	21	21	11	12.6	12.4	14.9	18.9	4.4	4.8	4

Table 1- (Continued)

	KESTANBOL GT					EYBEK GT						EVCİLER GT		
Sample No	ASM-K41	ASM-K42	ASM-K43	ASM-K44	ASM-K45	ASM-K64	ASM-K65	ASM-K66	ASM-K67	ASM-K69	ASM-K70	ASM-K34	ASM-K35	ASM-K36
SiO_2 (wt.%)	63.1	62.1	64.3	64.2	63.7	57.1	63.9	63.5	62.3	63.1	60.9	60.3	63.8	60.9
TiO_2	0.5	0.5	0.5	0.5	0.5	0.8	0.7	0.6	0.6	0.6	0.7	0.6	0.5	0.5
Al_2O_3	16.8	16.7	16.3	16.2	16.4	17.5	15.6	15.8	16.4	16.4	16.9	17.6	16.2	16.6
CaO	4.2	4.3	4	4	4.1	5.9	4.6	4.4	5	4.8	5.5	6	5	5.7
Fe_2O_3t	4.6	4.3	3.8	4	4	7.2	4.6	5	5.3	4.9	5.5	5.9	4.6	5.6
Na_2O	3.7	3.6	3.8	3.6	3.6	3.6	3	3.2	3.2	3.3	3.4	3.5	3.4	3.3
K_2O	4	4.7	4.5	4.5	4.4	2.8	4.2	3.8	3.6	3.5	3.4	3	3.1	2.9
MgO	1.7	2	1.5	1.6	1.7	2.7	2	2.2	2.1	2	2.4	1.9	1.7	2.5
MnO	0.1	0.1	0.1	0.1	0.1	0.1	0.1	0.1	0.1	0.1	0.1	0.1	0.1	0.1
P_2O_5	0.2	0.5	0.4	0.4	0.4	0.3	0.3	0.3	0.3	0.3	0.3	0.3	0.2	0.3
LOI	0.7	0.85	0.35	0.55	0.6	1.55	0.7	0.75	0.7	0.65	0.55	0.5	1.25	1.15
Total	99.6	99.65	99.55	99.65	99.5	99.55	99.7	99.65	99.6	99.65	99.65	99.7	99.85	99.55
A/CNK	0.93	0.89	0.88	0.90	0.90	0.89	0.87	0.91	0.90	0.91	0.88	0.88	0.90	0.88
A/NK	1.61	1.52	1.46	1.50	1.53	1.95	1.64	1.68	1.79	1.78	1.82	1.95	1.81	1.94
Sc (ppm)	12	15	14	12	16	17	14	14	16	13	20	13	11	11
V	140	138	118	124	125	4	4	4	4	4	5	145	129	137
Cr	81	127	106	107	127	10	15	21	25	21	24	105	157	136
Rb	151	213	205	186	193	136	163	166	164	141	164	107	112	87
Sr	393	819	793	770	788	1261	930	864	1039	899	1412	511	428	620
Y	18	21	23	21	14	19	42	25	24	20	26	26	20	20
Zr	22	14	10	10	12	25	13	10	11	10	13	7	6	6
Nb	13	18	18	16	15	12	6	5	6	5	7	12	11	9
Cs	7	7	8	4	4	9	4	5	5	5	4	6	3	3
Ba	844	1373	1116	1309	1301	618	1477	1079	1358	1068	1846	751	834	1145
La	46	52	31	29	22	37	66	56	63	50	65	54	59	53
Ce	92	102	65	60	45	71	151	109	118	93	123	106	109	98
Pr	10	10	7	6	5	8	19	12	13	11	14	11	10	10
Nd	36	40	30	25	21	34	78	49	53	43	58	40	38	36
Sm	6	7	6	5	4	6.3	14.4	8.6	9.1	7.8	10.4	7	6	6
Eu	1.62	1.92	1.48	1.35	1.45	1.7	2.6	1.9	2.2	1.9	2.9	1.81	1.61	1.52
Gd	6.8	7.9	5.7	5.3	4.4	6.5	14.5	9	9.1	8.2	10.8	7.9	6.9	6.3
Tb	0.81	0.94	0.84	0.72	0.56	0.8	1.8	1.1	1.1	0.9	1.3	1	0.8	0.78
Dy	3.8	4.4	4.6	4	2.7	4.3	9.1	5.2	5.2	4.5	6	5.1	3.8	3.8
Ho	0.69	0.78	0.85	0.77	0.51	0.7	1.4	0.8	0.8	0.7	0.9	0.98	0.69	0.71
Er	2.43	2.82	2.94	2.74	1.8	2.3	4.9	2.8	2.8	2.5	3.1	3.44	2.51	2.46
Tm	0.3	0.3	0.4	0.4	0.2	0.3	0.7	0.4	0.4	0.4	0.4	0.4	0.3	0.3
Yb	2	2.4	2.7	2.5	1.6	2.2	4.7	2.7	2.7	2.3	2.9	3	2.2	2.1
Lu	0.28	0.33	0.38	0.37	0.22	0.4	0.9	0.6	0.5	0.4	0.5	0.44	0.32	0.3
Hf	1.3	1.8	1.4	1.3	1.7	1.3	1.1	1	0.9	0.8	1	0.8	0.8	0.6
Ta	0.8	1.1	1.2	1.0	1.0	0.9	4.4	2.4	1.6	1.6	1.6	0.7	0.8	0.3
Pb	45	66	80	55	50	20	42	32	33	34	41	22	24	19
Th	134	109	78	78	76	0.8	3.1	2.5	2.3	2.1	1.7	138	147	133
U	31	26	24	25	23	12.2	27.3	20.4	14.9	14.3	11.1	31	28	27

Table 1- (Continued)

					ÇAMYAYLA GT					ALANKÖY GT			
Sample No	ASM-K37	ASM-K38	ASM-K39	ASM-K40	ASM-K20	ASM-K21	ASM-K22	ASM-K23	ASM-K24	ASM-K17	ASM-K18	ASM-K19	JG-1a (CRM Standard)
SiO_2 (wt.%)	75.2	73.8	64.6	64.8	63.4	62.1	64.5	63.8	63.8	65.7	66.3	65.2	
TiO_2	0.1	0.1	0.4	0.4	0.5	0.6	0.5	0.5	0.5	0.4	0.4	0.5	
Al_2O_3	14	14.4	15.9	16.1	16.9	16.3	17	17	17	16	16.3	16.5	
CaO	0.7	1.1	4.7	4.2	4	4.4	3.5	4.1	4	3.9	3.1	4.1	
Fe_2O_3t	0.8	1.2	4.3	3.9	4	4.3	3.8	4	4.2	3.9	3.8	4	
Na_2O	3.4	3.1	3.2	3.2	3.4	3.5	3.5	3.4	3.3	2.8	3.2	2.6	
K_2O	5	5.3	3.6	3.6	4	5	4.2	3.9	4.1	3.7	3.5	3.6	
MgO	0.2	0.3	1.8	1.7	1.8	2	1.5	1.7	1.6	1.6	1.4	1.6	
MnO			0.1	0.1	0.1	0.1	0.1	0.1	0.1	0.1	0.1	0.1	
P_2O_5			0.3	0.3	0.2	0.5	0.2	0.2	0.2	0.2	0.2	0.2	
LOI	0.3	0.35	0.75	1.6	1.45	0.7	0.95	0.8	0.9	1.4	1.4	1.35	
Total	99.7	99.65	99.65	99.9	99.75	99.5	99.75	99.5	99.7	99.7	99.7	99.75	
A/CNK	1.14	1.12	0.90	0.96	0.98	0.85	1.02	0.98	0.99	1.02	1.11	1.05	
A/NK	1.27	1.33	1.73	1.76	1.70	1.46	1.65	1.73	1.72	1.86	1.80	2.02	
Sc (ppm)	10	11	13	13	11	2	2	10	1	2	3	13	7
V	33	23	124	118	92	132	105	123	119	103	98	128	
Cr	204	162	158	236	66	144	75	80	92	145	145	92	
Rb	167	162	128	139	95	237	132	138	132	115	116	135	125
Sr	133	240	573	518	307	873	361	370	347	398	339	448	98
Y	18	19	21	20	15	9	11	19	9	11	10	23	35
Zr	13	11	5	5	10	10	21	9	10	15	12	12	92
Nb	8	8	10	9	11	21	14	14	14	11	9	12	
Cs	2	3	3	6	4	10	5	6	3	2	4	6	2
Ba	555	1030	1243	1030	725	1517	945	786	761	860	730	829	399
La	54	47	46	50	32	37	22	29	17	31	41	38	20.5
Ce	101	92	92	103	56	58	38	59	30	52	67	77	42
Pr	10	9	10	10	5	5	3	6	3	5	5	7	4.5
Nd	35	35	38	39	18	15	11	22	9	15	17	27	20
Sm	6	6	7	7	3	2	2	4	2	2	2	5	4
Eu	1.55	1.53	1.78	1.61	1.02	0.74	0.44	1.14	0.36	0.61	0.83	1.37	0.7
Gd	6.3	6.5	7.6	7.4	2.9	2.4	2	3.8	1.7	2.4	2.7	4.5	3.8
Tb	0.75	0.79	0.89	0.88	0.46	0.28	0.29	0.59	0.23	0.33	0.32	0.72	0.7
Dy	3.6	3.8	4.2	4.1	2.6	1.4	1.7	3.4	1.4	1.8	1.7	4.1	4
Ho	0.65	0.68	0.76	0.74	0.5	0.28	0.34	0.64	0.27	0.34	0.32	0.8	0.8
Er	2.29	2.39	2.68	2.65	1.75	1.03	1.26	2.26	1.04	1.29	1.19	2.81	2
Tm	0.3	0.3	0.3	0.3	0.2	0.1	0.2	0.3	0.2	0.2	0.2	0.4	0.3
Yb	2	2.1	2.2	2.3	1.6	1	1.5	2.1	1.2	1.4	1.1	2.5	3.5
Lu	0.29	0.29	0.31	0.31	0.24	0.15	0.23	0.31	0.19	0.2	0.17	0.37	0.4
Hf	0.7	0.6	0.6	0.6	0.8	0.9	1.3	0.7	0.7	1.3	1.1	1.1	2.9
Ta	0.7	0.6	0.7	0.7	0.7	1.3	0.9	0.9	0.8	0.9	0.6	0.8	2.5
Pb	23	23	28	20	18	89	41	32	19	84	17	66	
Th	150	114	124	168	80	61	76	79	66	85	66	94	15
U	28	25	26	32	20	15	17	21	17	20	16	22	4.1

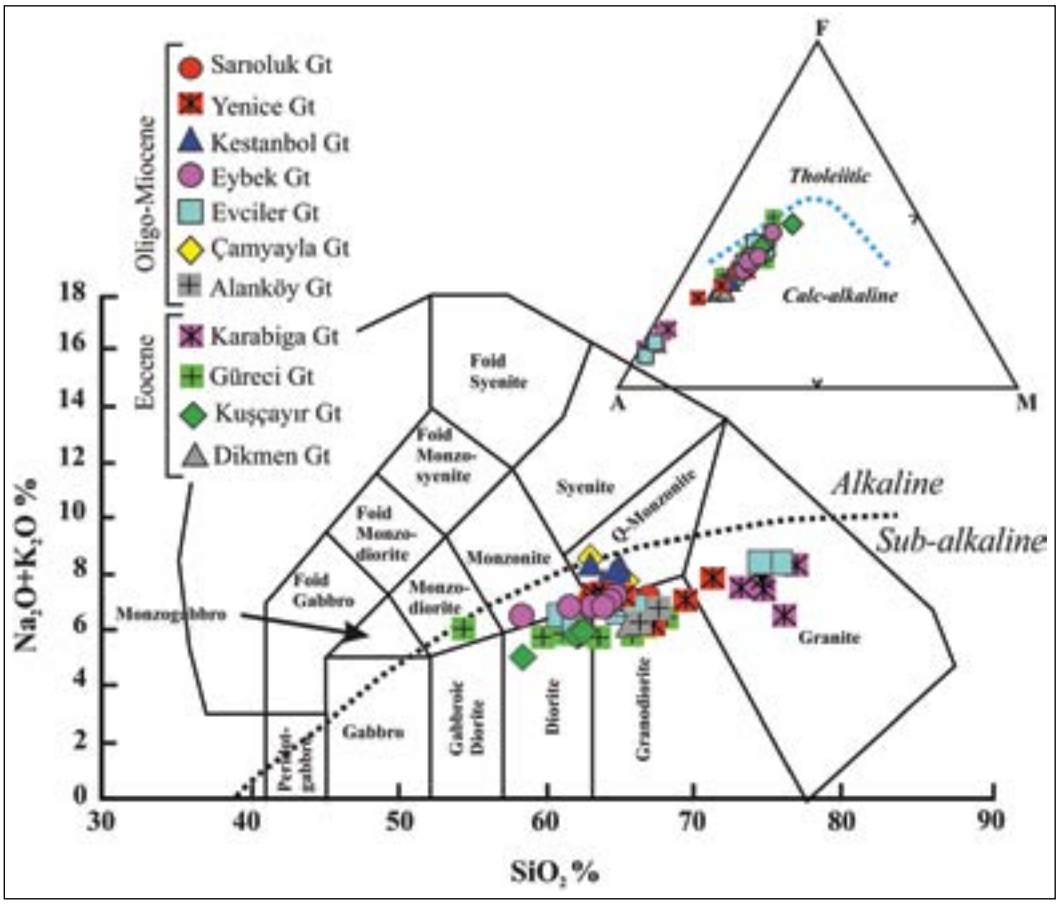

Figure 3- Total alkali-SiO_2 classification diagram for the Biga Peninsula granitoids (Middlemost, 1994). Insert figure is the AFM ternary diagram of Irvine and Baragar (1971); (A: Na_2O+K_2O, F: Fe_2O_3t, M: MgO)

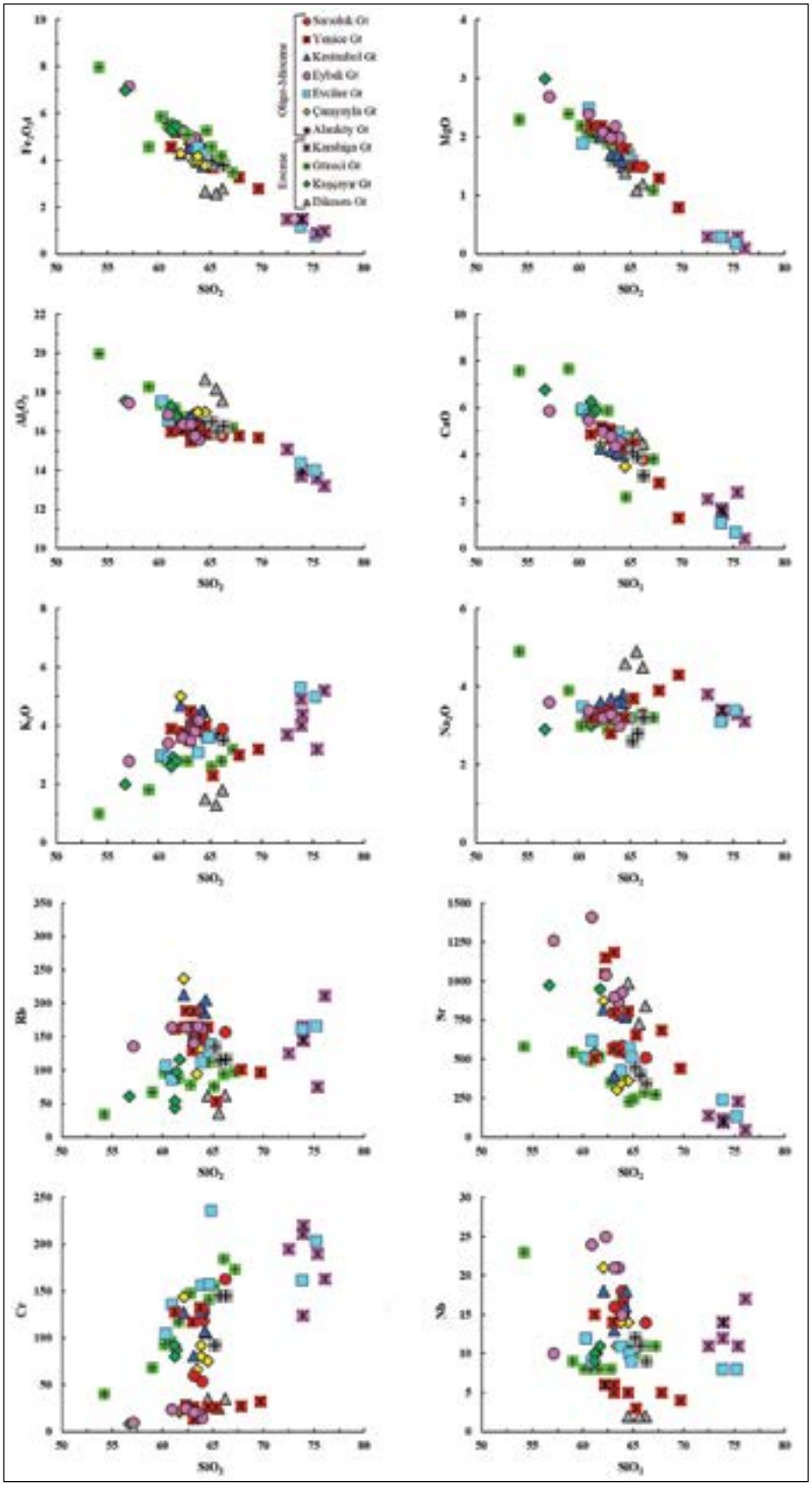

Figure 4- SiO_2 variation diagrams for the selected major-oxides and trace elements of the Biga Peninsula granitoids.

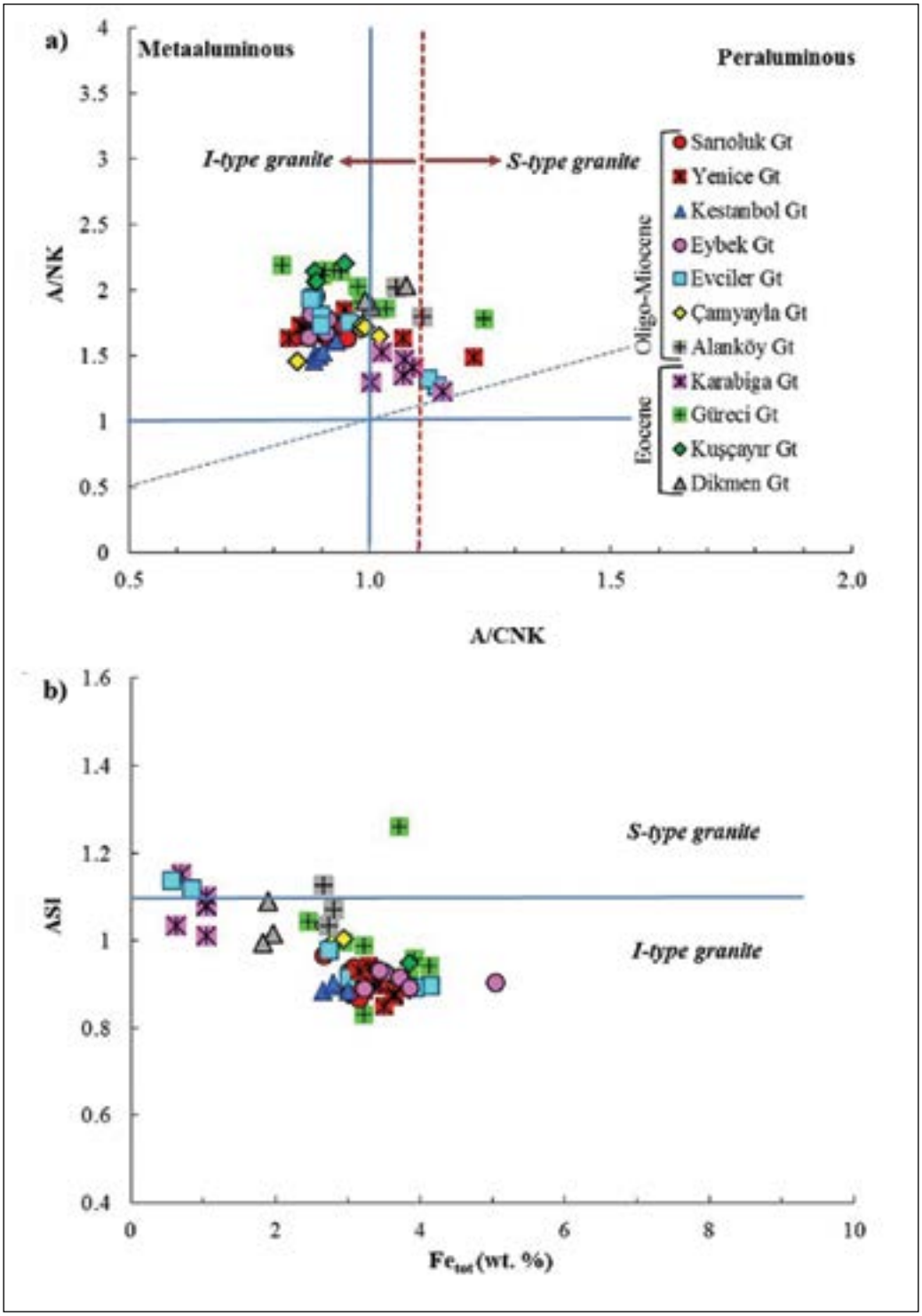

Figure 5- a) A/NK (molar) – A/CNK (molar) diagram (Shand, 1943); b) ASI (molar) – Fe_{tot} diagram (Norman et al., 1992) of the Biga Peninsula granitoids.

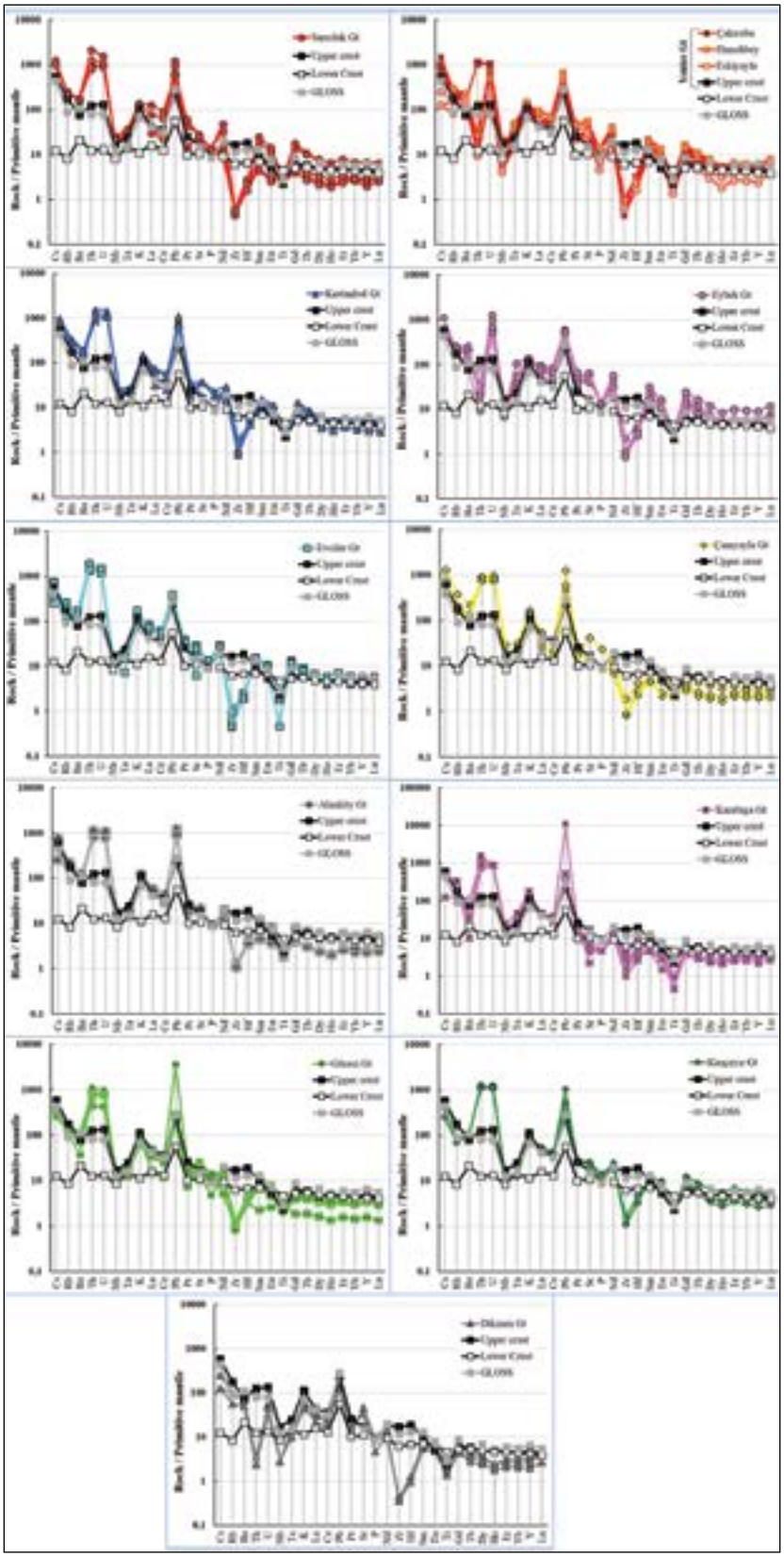

Figure 6- Primitive mantle normalised (Sun and McDonough, 1989) trace element patterns of Biga Peninsula granitoids. Upper crust, lower crust and GLOSS (*Global Subducting Sediment)* data are from Taylor and McLennan (1995), McLennan (2001) and Plank and Langmuir (1998).

material (Gill, 1981; Thompson et al., 1983; Fitton et al., 1988). In addition to above variations, while the Eocene Karabiga and Güreci granitoids have significant Th anomalies, Dikmen granitoids represent negative Th anomalies. Oligo-Miocene Sarıoluk, Yenice-Çakıroba, Kestanbol, Evciler, Çamyayla and Alanköy granitoids are characterised by significant Th positive anomalies, whereas Oligo-Miocene Yenice-Hamdibey, Yenice-Eskiyayla and Eybek granitoids are depleted in Th. Accordingly, the positive Th and U anomalies together with negative Nb, Ta and Ti anomalies may indicate the role of crustal/sediment contributions in the evolution of granitoids.

Figure 7 displays the chondrite-normalised (McDonough and Sun, 1995) rare earth element (REE) distribution diagrams of the selected samples from the Biga Peninsula granitoids. The great majority of the samples are enriched in light rare earth elements (LREE) relative to heavy rare earth elements (HREE) and they have $(La/Yb)_N$ ratios varying from 8 to 29. But, the low $[(La/Yb)_N = 2.17]$ ratio of a sample (ASM-K06) from Güreci granitoid can reflect the unfractionated nature of the sample. Most of the samples do not have significant negative Eu anomaly, but Karabiga and Sarıoluk granitoids have slight negative Eu anomaly, possibly indicating the fractionation of plagioclase (Figure 7).

6. Discussion

6.1. Identification of Magmatic Processes: Fractional Crystallization, Partial Melting and Crustal Contamination

Major oxide, trace element variation diagrams, trace and REE distribution patterns indicate that the Biga Peninsula granitoids were affected by fractional crystallisation processes during the evolution of the magmatism. But, the majority of samples had no clear negative Eu and Sr anomalies, indicating that plagioclase fractionation was not significant in the evolution of the Biga granitoids. As a result, in order to determine the effects of fractional crystallisation, the Rb-Sr and K/Rb-SiO_2 diagrams (Figure 8) is used, since Rb/Sr ratio is a good marker for fractional crystallisation and high Rb/Sr ratio indicates advanced degrees of fractionation (Imeokparia, 1981; Blevin, 2003). Most of the samples have Rb/Sr ratios varying from 0.1 to 1.0, whereas the Rb/Sr ratios in Karabiga

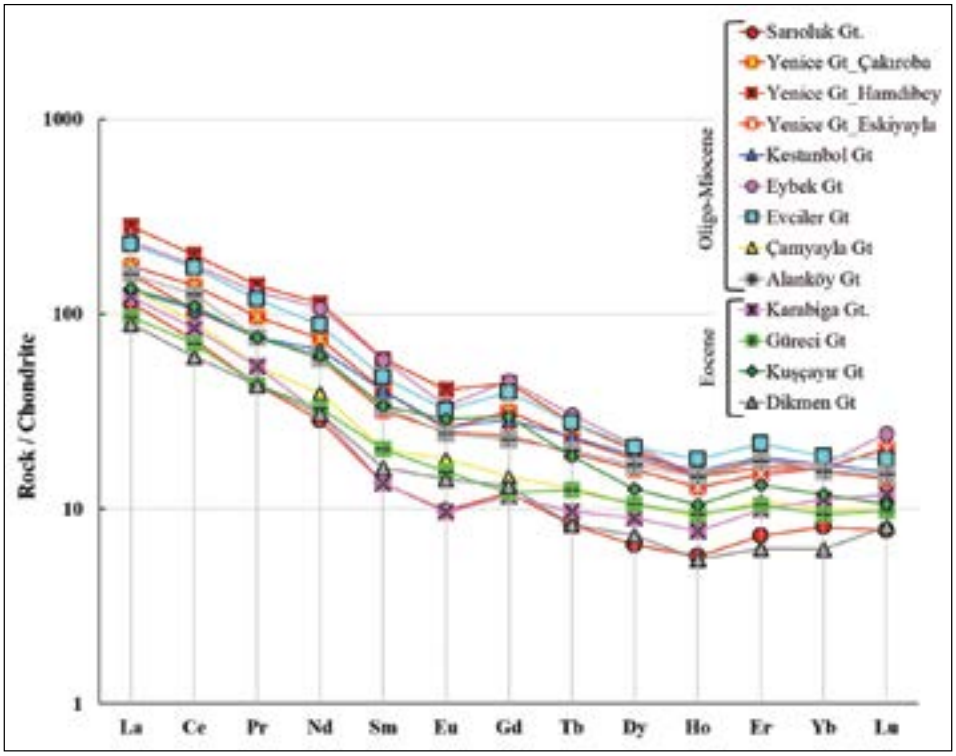

Figure 7- Chondrite normalised (McDonough and Sun, 1995) rare earth element patterns of the Biga Peninsula granitoids.

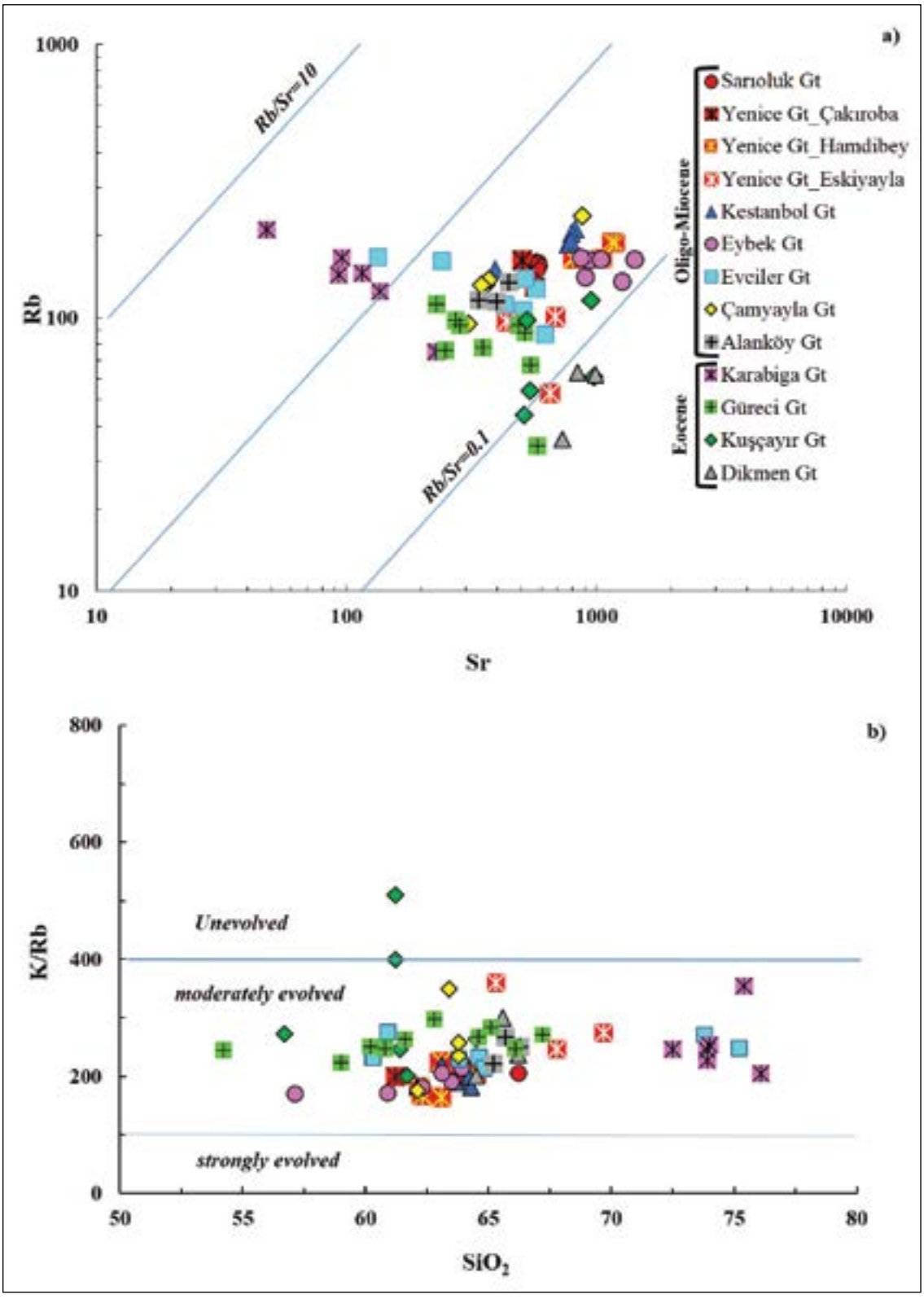

Figure 8- a) Rb-Sr and, b) K/Rb-SiO_2 diagrams (Blevin, 2003) for the Biga Peninsula granitoids.

and Dikmen samples range between 0.33-4.40 and 0.05-0.07, respectively (Figure 8a). Accordingly, while there is relatively strong fractionation for the Karabiga granitoids, the effects of this process are mildly in the Dikmen granitoids. Similarly, the K/Rb-SiO_2 diagram (Figure 8b) is one of the important indicators used to determine the degree of fractionation in granitic melts as low K/Rb and increasing SiO_2 content indicates strong fractionation (Blevin, 2003; Rossi et al., 2011). As seen on the figure 8b, the Biga Peninsula granitoids show moderate levels of fractionation.

The Rb-Ba-Sr triangular diagram adapted from El Bouseily and El Sokkary (1975) (Figure 9) (Karapetian et al., 2001; Xiang et al., 2017) is used to assess the magmatic differentiation process and tectonic setting features in the evolution of granitoids. The majority of samples display quartz diorite and granodiorite composition and are plotted in the I-type granite field, but the Karabiga granitoids fall in the area between S- and I-type granites and show strong fractionation (Figure 9). Samples having I-type granite characteristics show moderate level of fractionation. It can be concluded that the effects of the fractional crystallisation process were at moderate levels during the evolution of Biga Peninsula granitoids.Moreover, in order to asses the partial melting processes in the genesis of magmatism, the La – La/Yb diagram of Thirlwall (1994) is utilised (Figure 10). While horizontal trends give fractional crystallisation, the increasing La/Yb with increasing La indicates the partial melting processes. We conclude that partial melting is also thought to play a significant role.

Figure 8, 9 and 10 reveal the effects of fractional crystallisation and partial melting processes in the evolution and genesis of the magmatism. Besides, Ce/Pb – Pb and Rb/Ba – Rb/Sr diagrams were used to determine the effects of crustal contamination on magmatism (Figure 11). Low Ce/Pb ratio is one of the most characteristic features of crustal contribution and/or sediment contribution to mantle material because

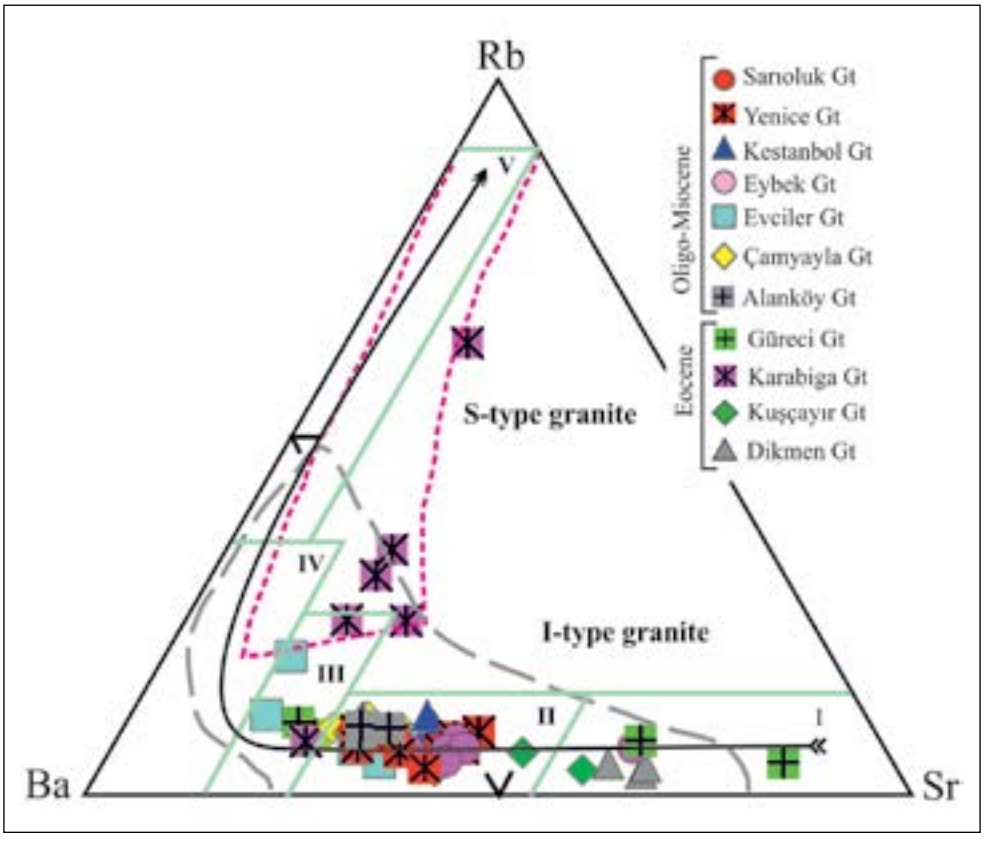

Figure 9- Rb-Ba-Sr ternary discrimination diagram of the Biga Peninsula granitoids (adapted from El Bouseily and El Sokkary, 1975; Karapetian et al., 2001 and Xiang et al., 2017). Roman numerals from I to V indicate poorly evolved granite to strongly evolved granite. I: Diorite; II. Granodiorite-Quartz-diorite; III. Anomalous granite; IV. Normal granite; V: strongly evolved granite.

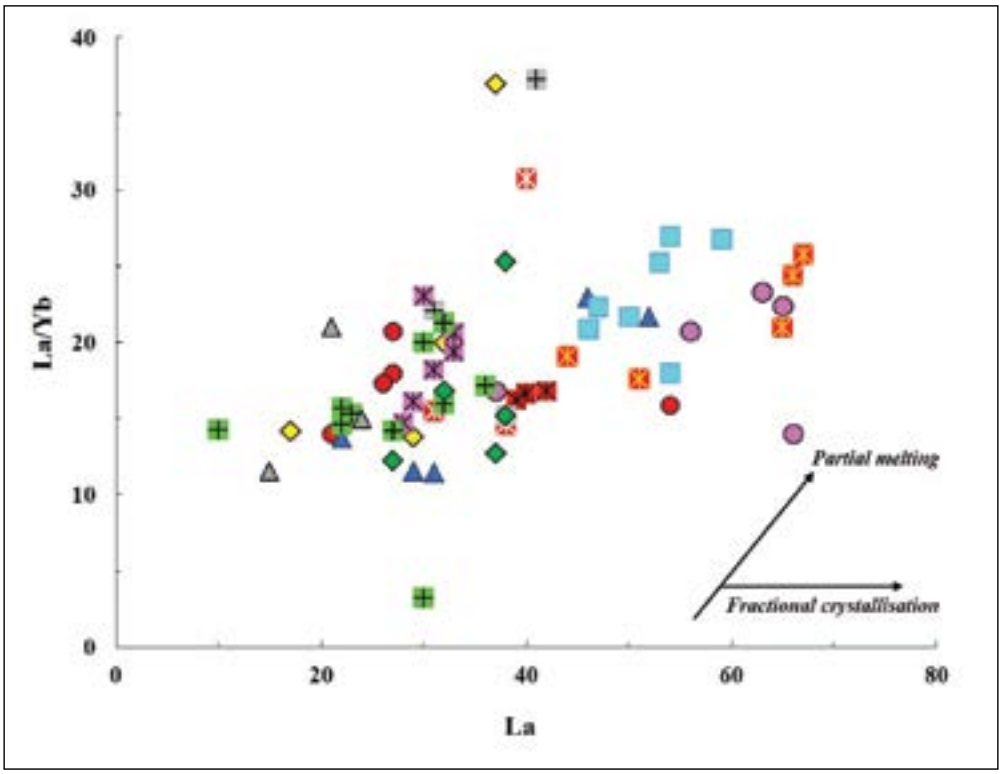

Figure 10- La – La/Yb diagram (Thirwall, 1994) of Biga Peninsula granitoids. Symbols as in figure 9.

the Pb content of crustal material is clearly higher compared to the mantle (Taylor and McLennan, 1985; Hofmann et al., 1986). Hofmann et al. (1986) showed that ocean island basalt (OIB) and mid-ocean ridge basalt (MORB) have high and relatively constant Ce/Pb ratios (~ 25), while the upper crust (UC) has lower Ce/Pb ratio (~3.2) (Taylor and Mc Lennan, 1985). In order to determine the role of crustal contamination in the evolution of Biga Peninsula granitoids, binary mixing modelling of Langmuir et al. (1978) was applied. In the mixing model, OIB&MORB and UC were used as end-members and two component binary mixing diagram between Pb and Ce/Pb were created. Biga Peninsula granitoids are plotted on the mixing curve between OIB&MORB and UC and shifted towards the UC end-member on the curve (Figure 11a).

Biga Peninsula granitoids show trace element distribution patterns similar to that of upper crust (Taylor and McLennan, 1985; McLennan, 2001) and GLOSS (Plank and Langmuir, 1998). But, there are some significant differences in detail. Sarıoluk, Yenice-Çakıroba, Kestanbol, Evciler, Çamyayla, Alanköy, Karabiga, Güreci and Kuşçayır granitoids are enriched in Th, whereas Yenice-Hamdibey, Yenice-Eskiyayla, Eybek and Dikmen granitoids are depleted in Th. Accordingly, high Th and Pb concentrations do not appear to be explained solely by crustal contamination processes. As a result, Rb/Ba – Rb/Sr diagrams has been used to distinguish the mantle-derived melts from crustal derived melts (Li et al., 2015; Chen et al., 2017) (Figure 11b). The diagram includes Sylvester (1998)'s basalt and pelite-derived melt curves. Most of the studied samples are plotted in the clay-poor source field but Karabiga samples are shifted towards the pelite-derived melt composition and clay rich source. According to this diagram (Figure 11b), derivation from crustal melting does not seem plausible explanation for the genesis of Biga Peninsula granitoids. Furthermore, although the crustal contribution may have played a role in the evolution of magmatism (Figure 11a), the negative anomalies in Nb, Ta and Ti and positive anomalies in Th and U, GLOSS-like trace element distributions and Rb/Ba-Rb/Sr variations essentially reflect the source characteristics rather than crustal contamination processes (Figure 11b).

Consequently, the observed geochemical variations – such as depletion in Nb, Ta, Ti, enrichment in Th,

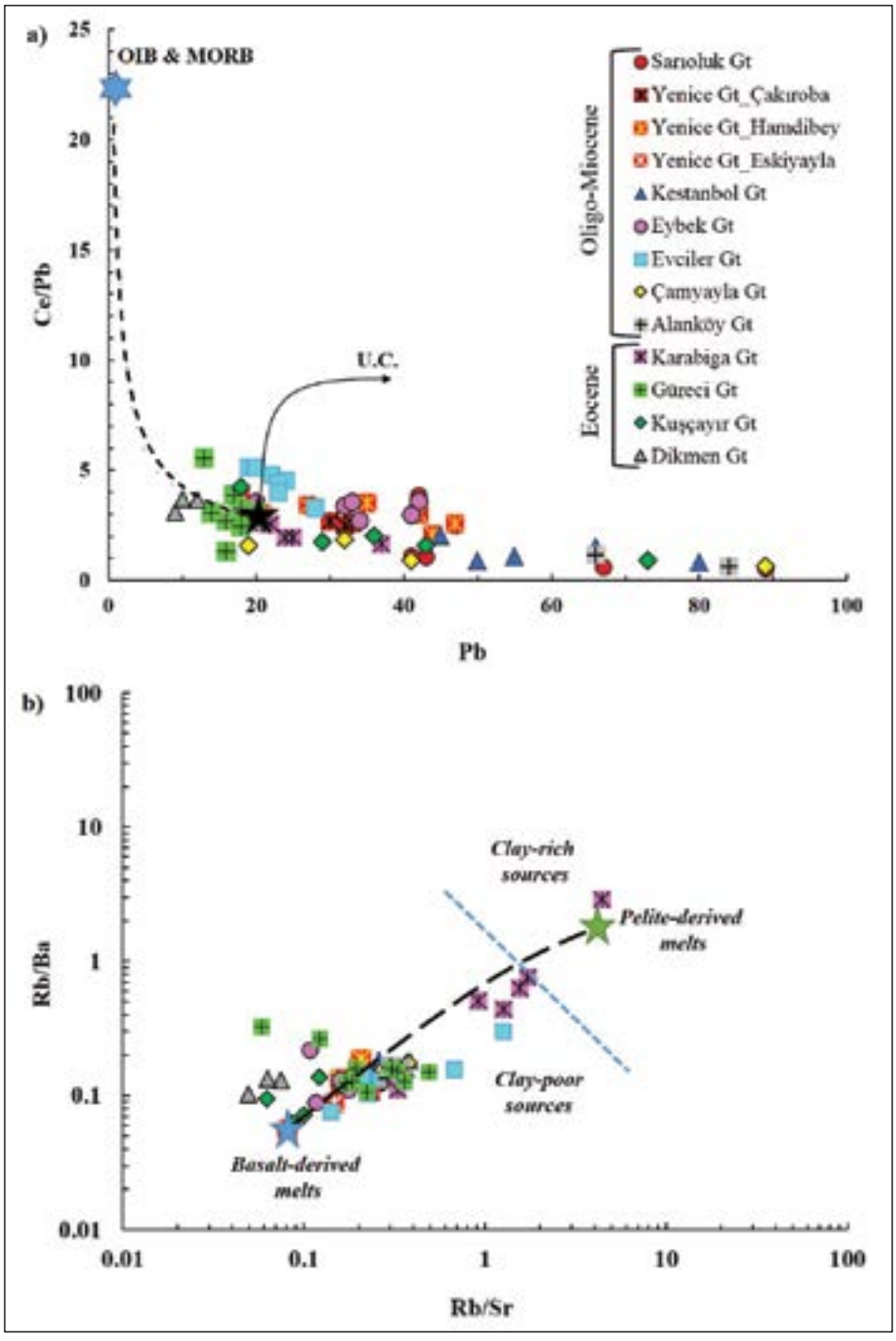

Figure 11- Biga Peninsula granitoids a) Ce/Pb – Pb binary mixing diagram. Binary mixing curve between OIB and MORB [average values of Normand and Garcia (1999)] and upper crust (UC) (Taylor and McLennan, 1985) is calculated from Langmuir et al. (1978); b) Rb/Ba – Rb/Sr diagram. Basalt- and pelite-derived melt curve from Sylvester (1998).

U and Pb and UC and GLOSS-like trace element distributions – are unlikely to be explained solely by crustal contamination. Because, magmas derived from mantle-source metasomatised by subduction components may retain these types of geochemical features. As a result, the source characteristics of the magmas generating the Biga Peninsula granitoids are assessed in the following section.

6.2. Tectonic Setting and Source Characteristics

In order to determine the tectonic setting of the Biga Peninsula granitoids, the tectonic discrimination diagram for granitic rocks of Pearce et al. (1984) is used (Figure 12). According to this diagram, samples are generally plotted in the volcanic arc granite (VAG) field. However, the tectonic setting of rocks falling at the intersection of within plate granites (WPG), arc granites (VAG) and syn-collisional granites (syn-COLG) is still controversial and this intersecting field is accepted as the post-collisional granite (post-COLG) field (Pearce, 1996). Accordingly, the Biga Peninsula granitoids can be clearly classified as post-collisional granites (Figure 12).

Nb/La – Ba/Rb and Ce/Pb – Ce diagrams have been used to reveal the role of subduction components on the samples exhibiting geochemical features similar to post-collisional granites (Figure 13). Low Nb/La and Ce/Pb ratios indicate subduction components. As can be clearly seen on the figures, the Biga Peninsula granitoids are plotted within the field represented by global subducted sediment (*GLOSS)*. According to these diagrams, the variatons in Nb/La, Ba/Rb and Ce/Pb can be attributed to subduction zone process and interpreted as that the post-collisional granitoids in the study area were derived from mantle source carrying subduction zone components.

In order to determine the process responsible for Th enrichment and the subduction components in Biga Peninsula granitoids, the element associations indicating different geochemical behaviour in aqeous fluid and sediment melt phases have been utilised. Ratios of slab-derived fluid/melt mobile elements (e.g. Th, Ba, Rb, Cs and La) to slab-derived fluid immobile element (e.g. Sm) are good markers for following the subduction zone components, since Ba, Rb and Cs elements mobilise with the aqueous fluid phases (McCulloch and Gamble, 1991; Ribiero et al., 2013), whereas Th and La are solely mobilise with sediment melting (Johnson and Plank, 1999; Ribeiro et al., 2013). Thus, Th/La and La/Sm are used by many researchers to determine the involvement of subducting sediment and sediment melts in subduction zones (Plank, 2005; Tommasini et al., 2011; Labanieh et al., 2012; Chen et al., 2017) and involvement of slab sediment into the overlying mantle wedge assigns the La/Sm ratios of the source (Labanieh et al., 2012). According to these criterion, La/Sm ratios (4.6-20.5) of almost

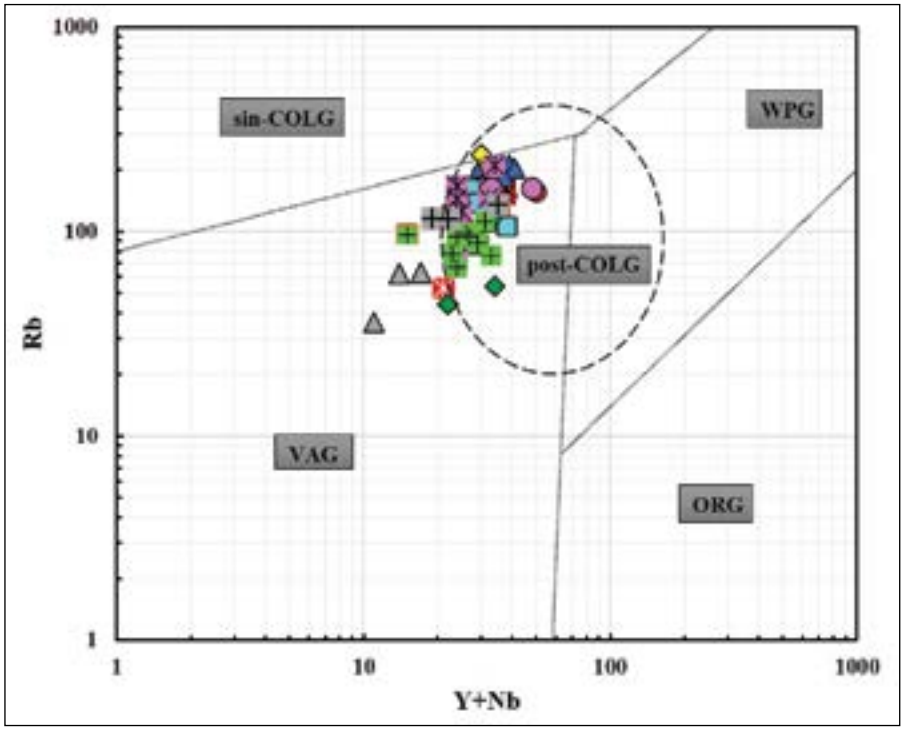

Figure 12- Rb- Y+Nb tectonic discrimination diagram of Biga Peninsula granitoids (Pearce et al., 1984; Pearce, 1996). VAG: Volcanic arc granites; syn-COLG: syn-collisional granites; WPG: within-plate granites; post-COLG: post-collisional granites. Symbols as in figure 11.

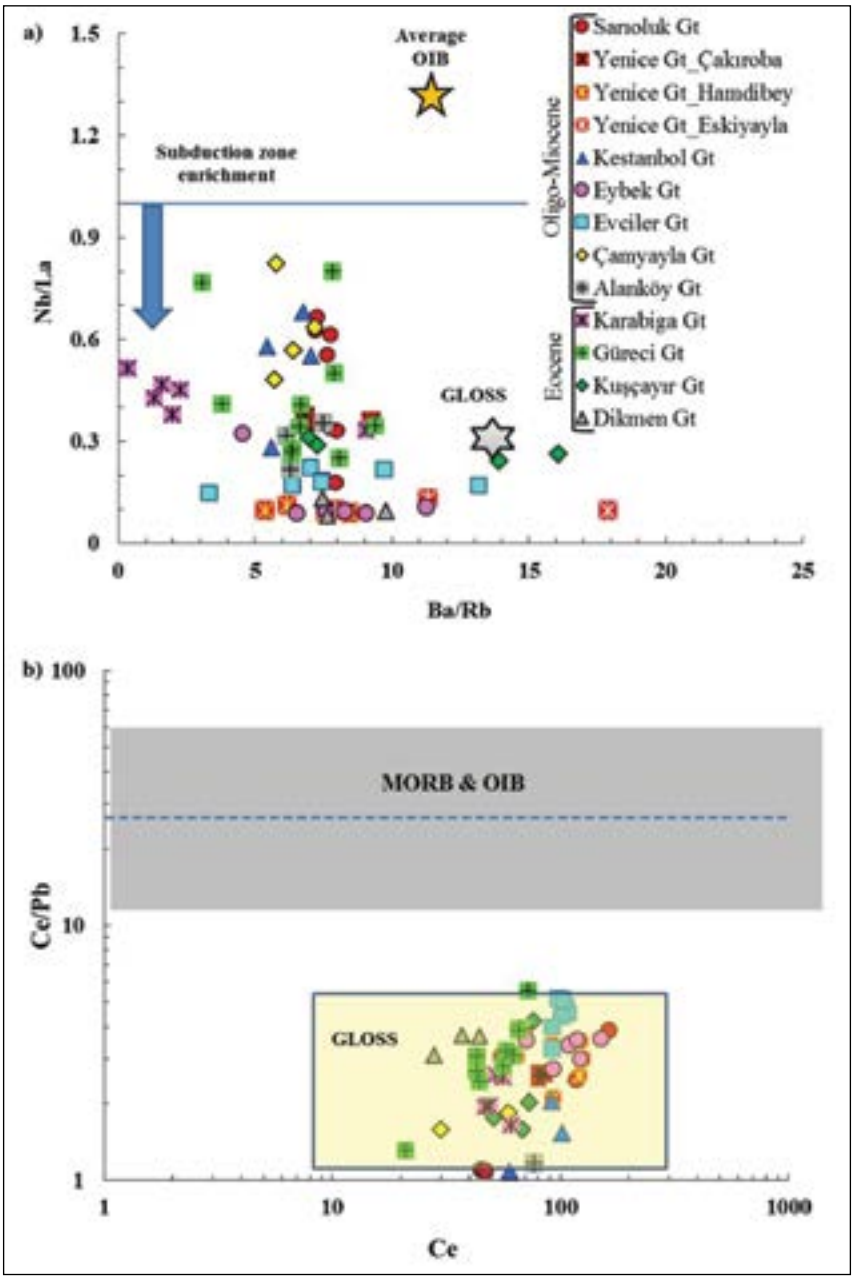

Figure 13- a) Nb/La-Ba/Rb (Wang et al., 2004) diagram of the studied samples. GLOSS (*Global Subducting Sediment*) values are from Plank and Langmuir (1998) and average OIB (Ocean island basalts) values are from Sun and McDonough (1989); b) Ce/Pb – Ce diagram of the studied samples. GLOSS field from Su et al. (2017) and references therein.

all samples and Th/La ratios (1.6-4.7) of Sarıoluk, Yenice-Çakıroba, Kestanbol, Evciler, Çamyayla, Alanköy, Karabiga, Güreci and Kuşçayır granitoids are sufficiently high to imply sediment involvement. But, La/Sm ratio also increase as a result of some processes such as weathering, fractional crystallisation and partial melting (Labanieh et al., 2012). As a result, to eliminate factors such as weathering and fractional crystallisation causing high La/Sm ratios in Biga Peninsula granitoids, the La/Sm – loss on ignition (LOI) and La/Sm - SiO_2 diagrams have been utilised (Figure 14). As the LOI values are directly related to degree of weathering, it increases with increasing weathering. Thus, LOI is a good marker to distinguish weathered sample from fresh sample (Chauvel et al., 2005). Labanieh et al. (2012) also demonstrate that

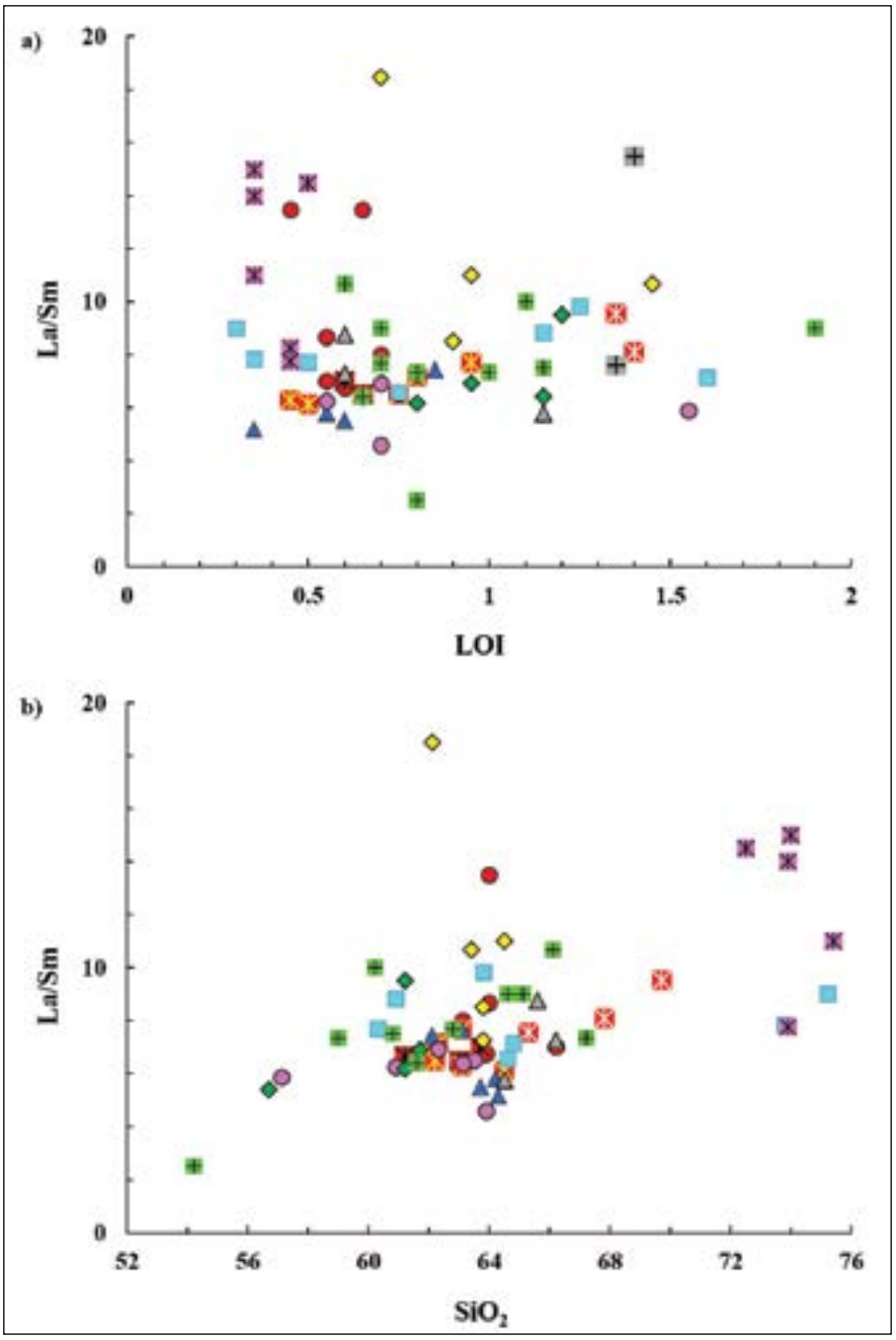

Figure 14- a) La/Sm – Loss on Ignition (LOI) and, b) La/Sm – SiO_2 diagrams of Biga Peninsula granitoids. Symbol as in figure 13.

La/Sm values increase with increasing weathering. As can be clearly seen on the figure 14a, there is no clear correlation between La/Sm and LOI. The lack of correlation between LOI and La/Sm indicates that weathering do not play a significant role on the ratio of La/Sm. In the plot of La/Sm versus SiO_2 (Figure 14b), there is a mild positive correlation with increasing SiO_2, but it does not adequate to explain the high La/Sm ratios in the samples. Consequently, the high La/Sm ratios (5-20) in Biga Peninsula granitoids can be attributed to sediment contribution (Labanieh et al., 2012).

Similarly, the Rb/Th, Cs/Th – La/Sm diagrams (Figure 15) are used to discriminate aqeous fluids from the sediment-derived melts in the samples (Ribeiro et

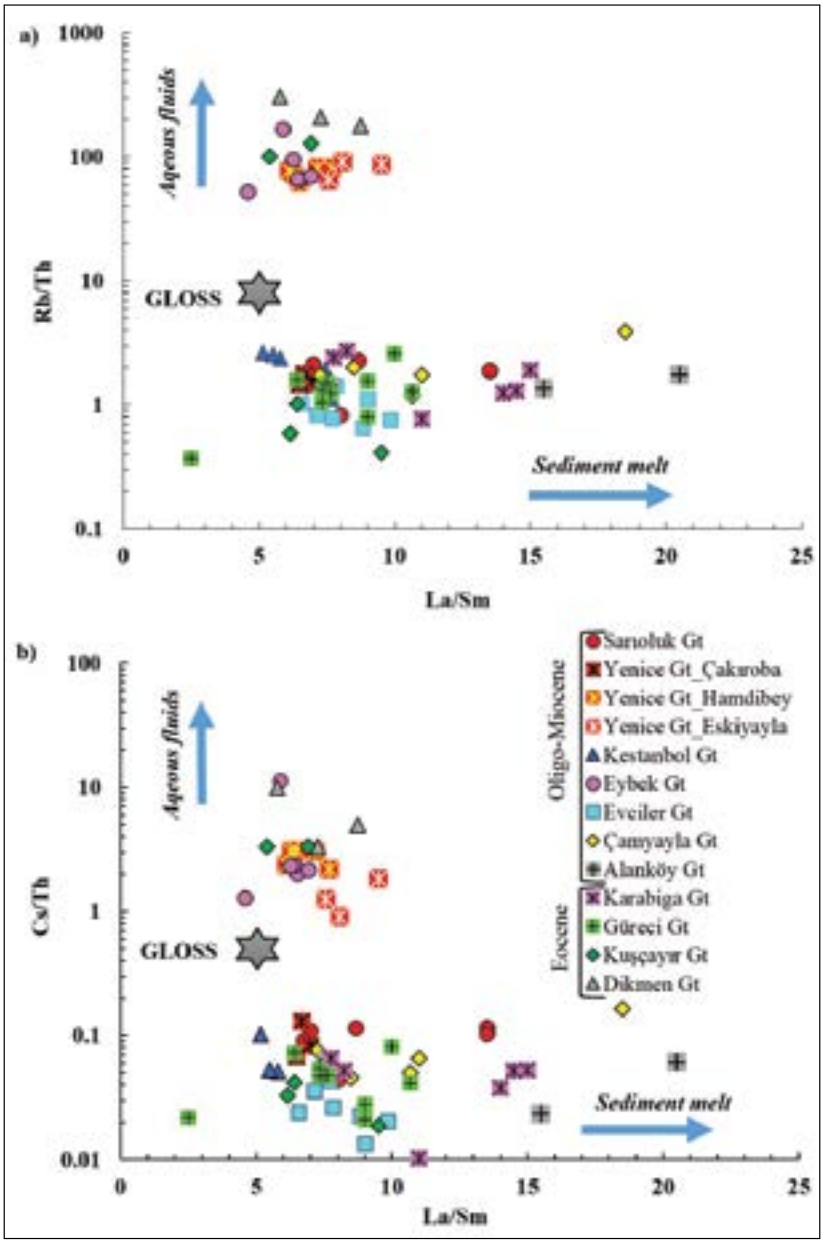

Figure 15- a) Rb/Th – La/Sm; b) Cs/Th – La/Sm diagrams (Ribeiro et al., 2013) of Biga Peninsula granitoids. GLOSS values from Plank and Langmuir (1998).

al., 2013). It can be interpreted that aqueous fluids were effective in the genesis of the Yenice-Hamdibey, Yenice-Eskiyayla, Eybek and Dikmen granitoids since they are characterised by low Th contents, whereas sediment melting appear to be the dominant process in the genesis of Th-enriched samples (Figure 15a, b).

6.3. Assesment of Ore-Formation Potential

Undoubtedly, granitic rocks and/or granitoids are very important in terms of ore potential. Many mineral deposits of economic significance are associated with granitic rocks, and the most important of these are copper (Cu)-molybdenum (Mo), Cu-Au, tin (S)-tungsten (W)-uranium (U) and rare metals (Ta-Cs-Li-Nb-Be-Sn-Mo-W) deposits. The Biga Peninsula, located in the Tethyan metallogenic belt containing the world's important ore deposits, is the most important metallogenic region in Turkey (Yiğit, 2012) As a result, to determine the mineralisation potential of Biga Peninsula granitoids, which have post-collisional features and exhibit both metaluminous

and peraluminous composition, and were derived from lithospheric mantle metasomatised by aqeous fluids and sediment melts, Ballouard et al.(2016)'s Nb/Th – Zr/Hf diagram has been used. Ballouard et al. (2016) suggested that peraluminous granites with low Nb/Ta ratios had experienced fluid interactions leading to enrichment in strongly incompatible elements such as Cs, Sn, F, Li, Rb and W and the Nb/Ta ratio may be used to distinguish barren granites from ore-bearing granites. They also demonstrated that low Nb/Ta content (<5) indicates concomitant effect of fractional crystallisation and magmatic-hydrothermal alteration, and F-rich acidic reduced fluids of magmatic origin are responsible for these types of processes. It is apparent on the Nb/Ta – Zr/Hf diagram (Figure 16), Yenice-Hamdibey and Eskiyayla, Eybek and Dikmen granitoids have low Nb/Ta and Zr/Hf contents and are shifted towards the rare metals related granites field. This case indicates that fluids of magmatic origin have played significant role in Dikmen, Eybek, Yenice-Hamdibey and Yenice-Eskiyayla granitoids and reflects the concomitant effect of fractional crystallisation along with magmatic-hydrothermal alteration. This is also supported by the observed variations in Rb/Th – La/Sm and Cs/Th – La/Sm diagrams (Figure 15) that aqeous fluids have played a significant role in the genesis of Yenice-Hamdibey and Yenice-Eskiyayla, Eybek and Dikmen granitoids.

7. Conclusions

Following the collision of the Sakarya continent with the Anatolide-Tauride platform in the Late Cretaceous-Early Tertiary, widespread magmatic activity developed in northwest Anatolia. Plutons in the Biga Peninsula are products of this magmatism and were emplaced in the time interval from the Eocene and Oligo-Miocene. The Biga Peninsula granitoids are products of a post-collisional environment, generating due to partial melting of a lithospheric mantle source metasomatised by aqueous fluids and sediment-melts released during the previous subduction. In addition, trace element distributions and trace element ratio diagrams demonstrate that crustal contamination and fractional crystallisation processes have also mildly effects in the evolution of the granitoids.

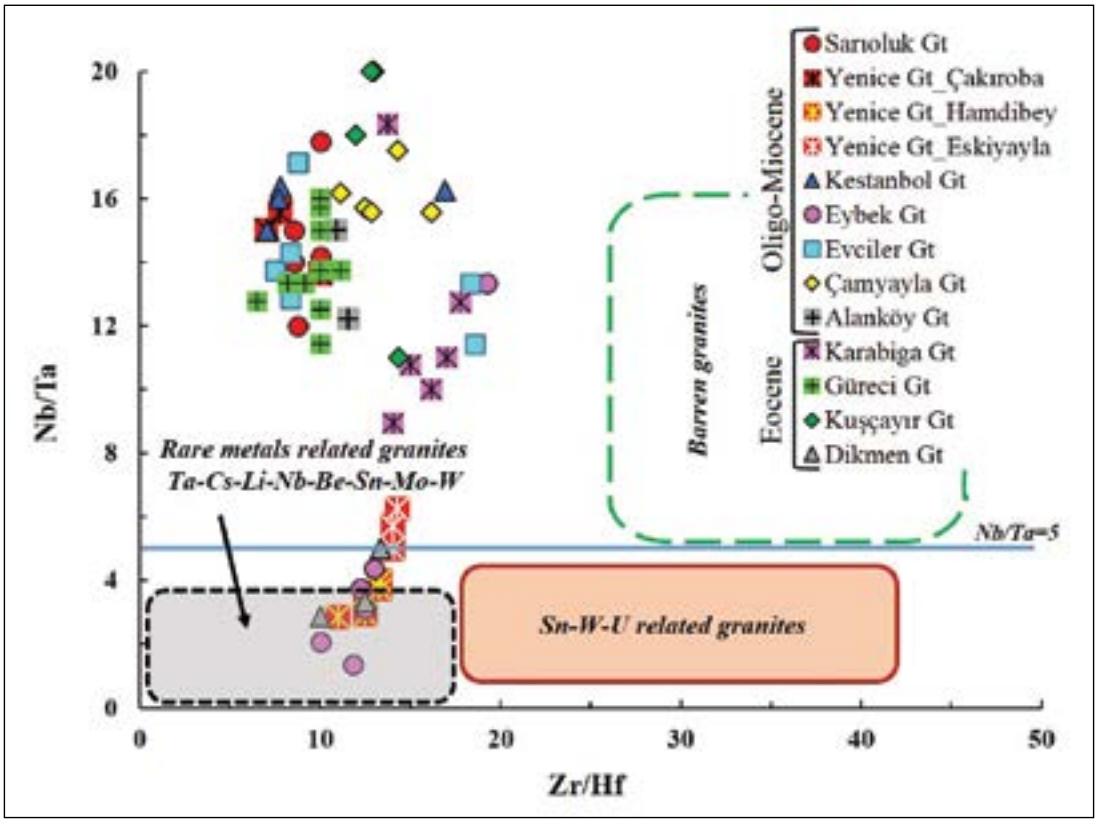

Figure 16- Nb/Ta-Zr/Hf diagram of diagram of Biga Peninsula granitoids (Ballouard et al., 2016).

Acknowledgements

This study was supported by the General Directorate of Mineral Research and Exploration (MTA) in the framework of the "Mineralisations related to acidic magmatism" project. We are extremely grateful to Mineral Research and Exploration Department and MTA northwestern Anatolia Region Headquarters (Balıkesir). We extend our special appreciation to S. Meltem Kadınkız and Nezihe Gökçe for their contributions in petrographical investigations. We are also grateful to Prof. Dr. Ahmet Gökçe and another anonymous reviewers for their constructive criticism and contributions to the final form of the manuscript.

References

Akyüz, H.S., Okay, A.İ. 1996. A section across a Tethyan Suture in Northwestern Turkey. International Geology Review 38, 405-418.

Aldanmaz, E., Pearce, J. A., Thirlwall,M.F., Mitchell, J. G. 2000. Petrogenetic evolution of late Cenozoic, post-collision volcanism in western Anatolia, Turkey. Journal of Volcanology and Geothermal Research, 102, 67– 95.

Aldanmaz, E., Pickard, M., Meisel, T., Altunkaynak, Ş., Sayıt, K., Şen, P., Hanan, B.B., Furman, T. 2015. Source components and magmatic processes in the genesis of Miocene to Quaternary lavas in western Turkey: constraints from HSE distribution and Hf–Pb–Os isotopes. Contribution to Mienarlogy and Petrology 170(2), 1-20.

Altıner, D., Koçyiğit, A., Farinacci, A., Nicosia, U., Conti, M.A. 1991. Jurassic– Lower Cretaceous stratigraphy and paleogeographic evolution of the southern part of northwestern Anatolia: Geologica Romana 28, 13–80.

Altunkaynak, Ş. 2007. Collision-driven slab breakoff magmatism in Northwestern Anatolia, Turkey. Journal of Geology 115, 63–82.

Altunkaynak, Ş., Dilek, Y. 2006. Timing and nature of postcollisional volcanism in western Anatolia and geodynamic implications. In: Dilek, Y., Pavlides, S. (Eds.), Post collisional tectonics and magmatism in the Mediterranean region and Asia: Geological Society of America Special Paper 409, 321–351.

Altunkaynak, Ş., Genç, Ş.C. 2008. Petrogenesis and time-progressive evolution of the Cenozoic continental volcanism in the Biga Peninsula, NW Anatolia (Turkey). Lithos 102, 316-340.

Altunkaynak, Ş., Dilek, Y. 2013. Eocene mafic volcanism in northern Anatolia: its causes and mantle sources in the absence of active subduction. International Geology Review 55 (13), 1641-1659.

Altunkaynak, Ş., Dilek, Y., Genç, Ş.C., Sunal, G., Gertisser, R., Furnes, H., Foland, K. A., Yang, J. 2012*a*. Spatial, temporal and geochemical evolution of Oligo-Miocene granitoid magmatism in western Anatolia, Turkey. Gondwana Research 21, 961-986.

Altunkaynak, Ş., Sunal, G., Aldanmaz, E., Genç, Ş.C., Dilek, Y., Furnes, H., Foland, K. A., Yang, J., Yıldız, M. 2012*b*. Eocene Granitic Magmatism in NW Anatolia (Turkey) revisited: New implications from comparative zircon SHRIMP U–Pb and 40Ar-39Ar geochronology and isotope geochemistry on magma genesis and emplacement. Lithos 155, 289-309.

Aysal, N. 2015. Mineral chemistry, crystallization conditions and geodynamic implications of the Oligo–Miocene granitoids in the Biga Peninsula, Northwest Turkey. Journal of Asian Earth Science 105, 68-84.

Ballouard, C., Pojol, M., Boulvais, P., Branquet, Y., Tartese, R., Vigneresse, J-L. 2016. Nb-Ta fractionation in peraluminous granites: A marker of the magmatic-hydrothermal transition. Geology 44(3), 231-234.

Blevin, P. 2003. Metallogeny of granitic rocks, The Ishihara Symposium, Granites and Associated Metallogenesis 14, 5-80.

Chauvel, C., Dia, A. N., Bulurde, M., Chabaux, F., Durand, S., Ildefonse, P., Gerard, M., Deruelle, B., Ngounouno, I. 2005. Do decades of tropical rainfall affect the chemical compositions of basaltic lava flows in Mount Cameroon? Journal of Volcanology and Geothermal Research 141, 195-223.

Chen, B., Long, X., Wilde S.A., Yuan, C., Wang, Q., Xia, X., Zang, Z. 2017. Delamination of lithospheric mantle evidenced by Cenozoic potassic rocks in Yunnan, SW China: A contribution to uplift of the Eastern Tibetan Plateau. Lithos 284-285, 709-729.

Delaloye, M., Bingöl, E. 2000. Granitoids from western and northwestern Anatolia: geochemistry and modeling of geodynamic evolution. International Geology Review 42, 241– 268.

Dilek, Y. 2006. Collision tectonics of the Mediterranean region: causes and consequences. Geological Society of America, Special Paper 409, 1-13.

Dilek, Y., Altunkaynak, Ş. 2009. Geochemical and temporal evolution of Cenozoic magmatism in western

Turkey: mantle response to collision, slab break-off, and lithospheric tearing in an orogenic belt. Geological Society, London, Special Publications 311, 213-233.

Duru, M., Pehlivan, Ş., Okay, A.İ., Şentürk, Y., Kar, H. 2012. Biga Yarımadası'nın Tersiyer öncesi jeolojisi. Biga Yarımadası'nın Genel ve Ekonomik Jeolojisi MTA Özel Yayın Serisi-28, 7-77.

El Bouseily, A.M., El Sokkary, A.A. 1975. The relation between Rb, Ba and Sr in granitic rocks. Chemical Geology 16, 207-219.

Ercan, T., Satır, M., Steinitz, G., Dora, A., Sarıfakıoğlu, E., Adis, C., Walter, H.J., Yıldırım, T. 1995. Biga Yarımadası ile Gökçeada, Bozcaada ve Tavşan adalarındaki KB Anadolu Tersiyer volkanizmasının özellikleri. Bulletin of Mineral Research and Exploration 117, 55-87.

Erkül, S.T., Erkül, F. 2012. Magma interaction processes in syn-extensional granitoids: the Tertiary Menderes Metamorphic core complex, western Anatolia, Turkey. Lithos 142-143, 16-33.

Ersoy, E.Y., Palmer, M.R. 2013. Eocene–Quaternary magmatic activity in the Aegean: implications for mantle metasomatism and magma genesis in an evolving orogeny. Lithos 180-181, 5–24.

Ersoy, E.Y., Palmer, M.R., Can Genç, Ş., Prevelic D., Akal, C., Uysal, İ., 2017*a*. Chemo-probe into the mantle origin of the NW Anatolia Eocene to Miocene volcanic rocks: Implications for the role of, crustal accretion, subduction, slab roll-back and slab break-off processes in genesis of post-collisional magmatism. Lithos 288-289, 55-71.

Ersoy, E.Y., Akal, C., Can Genç, Ş., Candan, O., Palmer, M.R., Prelevic, D., Uysal, İ., Mertz-Kraus, R., 2017*b*. U-Pb zircon geochronology of the Paleogene-Neogene volcanism in the NW Anatolia: Its implications for the late Mesozoic-Cenozoic geodynamic evolution of the Aegean. Tectonophysics 717, 284-301.

Fitton, J. G., James, D., Kempton, P.D., Ormerod, D.S. Leeman, W.P. 1988. The role of lithospheric mantle in the generation of late Cenozoic basic magmas in the Western United States. Journal of Petrology Special Lithosphere Issue 331-349.

Genç, Ş. C. 1998. Evolution of the Bayramiç magmatic complex. Journal of Volcanology and Geothermal Research, 85 (1- 4), 233-249.

Genç, Ş. C., Yılmaz, Y. 1997. An example of Post-collisional Magmatism in Northwestern Anatolia: the Kızderbent Volcanics (Armutlu peninsula, Turkey). Turkish Journal of Earth Science 6, 33-42.

Genç, Ş. C., Altunkaynak, Ş. 2007. Eybek graniti (Biga yarımadası, KB Anadolu) üzerine: Yeni jeokimya verileri ışığında yeni bir değerlendirme. Yerbilimleri 28 (2), 75-98.

Gill, J.B. 1981. Orogenic andesites and Plate tectonics. Springer - Verlag, New York.

Güleç, N. 1991. Crust-mantle interaction in western Turkey: implications from Sr and Nd isotope geochemistry of Tertiary and Quaternary volcanics. Geological Magazine 123, 417-435.

Gülmez, F., Genç, Ş.C., Keskin, M., Tüysüz, O. 2013. A post-collision slab-breakoff model for the orgin of the Middle Eocene magmatic rocks of the Armutlu-Almacık belt, NW Turkey and its regional implications. Geological Society, London, Special Publications 372, 107-139.

Harris, N.B.W., Kelley, S., Okay, A.İ. 1994. Post-collsion magmatism and tectonics in northwest Anatolia. Contributions to Mineralogy and Petrology 117, 241-252.

Hasözbek, A., Satır, M., Erdoğan, B., Akay, E., Siebel, W. 2010*a*. Early Miocene granite formation by detachment tectonics or not? A case study from the northern Menderes Massif (Western Turkey). Journal of Geodynamics 50, 67–80.

Hasözbek, A., Satır, M., Erdoğan, B., Akay, E., Siebel, W. 2010*b*. Early Miocene postcollisional magmatism in NW Turkey: geochemical and geochronological constraints. International Geology Review 53, 1098–1119.

Hofmann, A.W., Jochum, K.P., Seufer, M., White W.M. 1986. Nb and Pb in oceanic basalts: new constraints on mantle evolution. Earth and Planetary Science Letters 79, 33-45.

Ilgar, A., Sezen Demirci, E., Demirci, Ö. 2012. Biga Yarımadası Tersiyer istifinin stratigrafisi ve sedimantolojisi. Biga Yarımadası'nın Genel ve Ekonomik Jeolojisi Maden Tetkik ve Arama Genel Müdürlüğü Özel Yayın Serisi-28, 75-120.

Imeokparia, E.G. 1981. Ba/Rb and Rb/Sr ratios as indicators of magmatic fractionation, postmagmatic alteration and mineralization-Afu Younger Geranite Complex, Northern Nigeria. Geochemical Journal 15, 209-219.

Irvine, T. N., Baragar, W. R. A. 1971. A guide to the chemical classification of the common volcanic rocks. Canadian Journal of Earth Science 8, 523-548.

Johnson, M.C., Plank, T., 1999. Dehydration and melting experiments constrain the fate of subducted sediments. Chemical Geology 130, 289-299.

Karacık, Z., Yılmaz, Y. 1998. Geology of the ignimbrites and the associated volcano–plutonic complex of the Ezine area, northwestern Anatolia. Journal of Volcanology and Geothermal Research 85(1), 251-264.

Karacık, Z. Yılmaz, Y., Pearce, J., Ece, Ö.I. 2008. Petrochemistry of the South Marmara granitoids, northwest Anatolia, Turkey. International Journal of Earth Science 97, 1181-1200.

Karapetian, S.G., Jrbashian, R.T., Mnatsakanian A.K. 2001. Late collision rhyolitic volcanism in the north-eastern part of Armenian Highland: Journal of Volcanology and Geothermal Research 112, 189-220.

Keskin, M., Genç, Ş.C., Tüysüz, O. 2008. Petrology and geochemistry of post-collisional Middle Eocene volcanic units in North-Central Turkey: Evidence for magma generation by slab breakoff following the closure of the Northern Neotethys Ocean. Lithos 104, 267-305.

Konak, N., Alan, İ., Bakırhan, B., Bedi, Y., Dönmez, M., Pehlivan, Ş., Sevin, M., Türkecan, A., Yusufoğlu, H. 2016. 1/1.000.000 Ölçekli Türkiye Jeoloji Haritası. Maden Tetkik ve Arama Genel Müdürlüğü Yayını, Ankara-Türkiye.

Köprübaşı, N., Aldanmaz, E. 2004. Geochemical constraints on the petrogenesis of Cenozoic I-type granitoids in Northwest Anatolia, Turkey: evidence for magma generation by lithospheric delamination in a post-collisional setting. International Geology Review 46, 705–729.

Köprübaşı, N., Şen, C., Köprübaşı, N. 2000. Geochemistry of Fıstıklı (Armutlu–Yalova) granitoid. Bulletin of Earth Sciences Application and Research Centre of Hacettepe University, 22, 33–42.

Kürkcüoğlu, B., Furman, T., Hannan, B. 2008. Geochemistry of post-collisional mafic lavas from the North Anatolian Fault zone, Northwestern Turkey. Lithos 101, 416-434.

Labanieh, S., Chauvel, C., Germa, A., Q., X. 2012. Martinique: a clear case for sediment melting and slab dehydration as a function of distance to the trench. Journal of Petrology 53 (12), 2411-2464.

Langmuir, C.H., Vocke, R.D., Hanson, G.N., Hart, S.R. 1978. A general mixing equation with applications to İcelandic basalts. Earth and Planetary Science Letters 37, 380-392.

Li, D., He, D., Fan, C. 2015. Geochronology and Sr-Nd-Hf isotopic composition of the granites, enclaves, and mafic dykes in the Karamaya area, NW China: Insights into late Carboniferous crustal growth of West Junggar. Geoscience Frontiers 6 (2), 153-173.

Maniar, P. D., Piccoli, P.M. 1989. Tectonic discrimination of granitoids. Geological Society of America Bulletin 101, 635–643.

McDonough, W.F., Sun, S.S. 1995. The composition of the Earth. Chemical Geology 120, 223-253.

McCulloch, M.T., Gamble, J.A. 1991. Geochemical and geodynamical constraints on subduction zone magmatism. Earth and Planetary Science Letter 102, 358-374.

McLennan, S.M. 2001. Relationship between the trace element composition of sedimenatry rocks and upper continental crust. Geochemistry Geophysics Geosystems 2, article no. 2000GC000109.

Middlemost, E. A. K. 1994. Naming materials in magma/igneous rock system. Earth-Science Reviews 37, 215-224.

Normand, M.D., Garcia, M.O. 1999. Primitive magmas and source characteristivs of the hawaiian plume: petrology and geochemistry of shield picrites. Earth and Planetary Science Letters 168, 27-44.

Normand, M. D., Leeman, W. P., Mertzman, S. A. 1992, Granites and rhyolites from the northwestern USA: Temporal variation in magmatic processes and relations To tectonic setting: Transactions of the Royal Society of Edinburgh, Earth Science 83, 71–81.

Okay, A.İ. 1989. Tectonic units and sutures in the pontides, Northern Turkey. *In*: Sengör AMC (ed) Tectonic evolution of the Tethyan region, Kluwer academic publishers, pp 109-116.

Okay, A.İ. 2008. Geology of Turkey: A synopsis, Anschitt 21, 19-42.

Okay, A.İ., Tüysüz, O. 1999. Tethyan sutures of northern Turkey. In: Durand, B., Jolivet, L., Horvath, F., Seranne, M. (Eds.), The Mediterranean Basin: Tertiary Extansion within the Alpine Orogen, 156. Geological Society, Special Publications, London, pp. 75– 515.

Okay A.İ., Göncüoğlu, M.C. 2004. Karakaya Complex: A review of data and concepts. *Turkish Journal of Earth Sciences* 13: 77-95.

Okay, A.İ., Satır, M. 2006. Geochronology of Eocene plutonism and metamorphism in northest Turkey: evidence for a possible magmatic arc. Geodinamica Acta 19, 251– 266.

Okay, A.İ., Satır, M., Maluski, H., Siyako, M., Monie, P., Metzger, R., Akyüz, S. 1996. Palaeo- and Neo-Tethyan events in northwest Turkey. *In* Yin E & Harrison M (eds) Tectonics of Asia, Cambridge University Press, 420-441.

Okay, A.İ., Tansel, İ., Tüysüz, O. 2001. Obduction, subduction and collsion as reflected in the Upper Cretaceous-Lower Eocene sedimentary record of western Turkey. Geological Magazine 138(2), 117-142.

Okay, A.İ., Satır, M., Siebel, W. 2006. Pre-Alpide Palaezoic and Mesozoic orogenic events in the Eastern Mediterranean region. In: Gee, D.G. & Stephenson, R.A. (eds), European Lithosphere Dynamics. Geological Society, London, Memoirs 32, 389-405.

Pearce, J.A. 1996. Sources and settings of granitic rocks. Episodes 19 (4), 120-125.

Pearce, J.A., Harris, N.B.W., Tindle, A.G. 1984. Trace element discrimination diagrams for the tectonic interpretation of granitic rocks. Journal of Petrolology 25, 956-983.

Peccerillo, A., Taylor, S.R. 1976. Geochemistry of Eocene calcalkaline volcanic rocks from the Kastamonu area, northern Turkey. Contributions to Mineralogy and Petrology 58, 63–81.

Plank, T. 2005. Constraints from thoriıum/lanthanum on sediment recycling at subduction zones and the evolution of the continents. Journal of Petrology 46 (5), 921-944.

Plank, T., Langmuir, C.H. 1998. The chemical composition of subducting sediment and its consequences for the crust and mantle. Chemical Geology 145, 325-394.

Poutiainen, M., Scherbakov, T.F. 1998. Fuid and melt inclusion evidence fort he origin of idiomophic quartz crystals in topaz-bearing granite from the Salmi batholih, Karelia, Russia. Lithos 44, 141-151.

Ribeiro, J. Stern, R.J., Kelley, K.A., Martinez, F., Ishizuka, O., Manton, W.I., Ohara, Y. 2013. Nature and distribution of slab-derived fluids and mantle sources beneath the Southeast Mariana forearc rift. Geochemistry Geophysics Geosystems 14, 4865-4607, doi:10.1002/ggge.20244.

Rossi, J.N., Toselli, A.J., Basei, M.A., Sial, A.N., Baez, M. 2011. Geochemival indicators of metalliferpus fertility in the Carboniferous San Blas pluton, Sierra de Velasco, Argentina. In: Sial, A. N., Bettencourt, J. S., De Campos, C. P. & Ferreira, V. P. (eds), Granite-Related Ore Deposits. Geological Society, London, Special Publications 350, 175–186.

Seyitoğlu, G., Scott, B.C. 1996. The cause of N-S extensional tectonics in West Turkey. Tectonic escape vs. Back-arc spreading vs. Orogenic collapse. Journal of Geodynamics, 22, 145 - 153.

Shand, S.J. 1943. The eruptive rocks: 2nd edition, John Wiley, New York, 444 p.

Su, H-M., Jiang S-Y., Zhang, D-Y., Wu, X-K. 2017. Partial Melting of Subducted Sediments Produced Early Mesozoic Calc-alkaline Lamprophyres from Northern Guangxi Province, South China. Scientific Reports 7: 4864 (DOI:10.1038/s41598-017-05228-w).

Sun, S.S., McDonough, W.F. 1989. Chemical and isotopic systematics of oceanic basalts: implications for mantle composition and processes. In: Saunders, A.D. and Norry, M.J. (eds.), Magmatism in ocean basins. Geological Society of London Special Publication 42, 313-345.

Sylvester, P.J., 1998. Post-collisional strongly peraluminous graites. Lithos 45, 29-44.

Şengör, A.M.C., Yılmaz, Y. 1981. Tethyan evolution of Turkey: a plate tectonic approach. Tectonophysics, 75, 181-241.

Taylor S., R., Mc Lennan, S.M. 1985. The continental crust: its composition and evolution. An examination of the geochemical record preserved in sedimentary rocks. Blackwell Scientific Publications 46, pp.838.

Thompson R. N., Morrison M. A., Dickin A. P., Hendry, G. L. 1983. Continental flood basalts… Arachnids rule OK?, *in* Hawkesworth, C. J., and Norry, M. J. (eds.), Continental basalts and mantle xenoliths: Nantwich, UK, Shiva, 158–185.

Tommasini, S., Avanzinelli, R., Conticelli, S. 2011. The Th/La and Sm/La conundrum of the Tethyan realm lamproites. Earth and Planetary Science Letters 301, 469-478.

Topuz, G., Altherr, R., Schwartz, W.H., Dokuz, A., Meyer, H.-P. 2007. Variscan amphibolites-facies rocks from the Kurtoğlu metamorphic complex (Gümüşhane area, Eastern Pontides, Turkey). International Journal of Earth Science 96, 861–873.

Ustaömer, P.A., Ustaömer, T., Collins, A.S., Reischpeitsch, J. 2009. Lutetian arc-type magmatism along the southern Eurasian margin: new U–Pb LA-ICPMS and whole-rock geochemical data from Marmara Island, NW Turkey. Mineralogy and Petrology 96, 177– 196

Wang, K.-L., Chung, S.-L., O'Reilly, S. 2004. Geochemical Constraints for the Genesis of Post-collisional Magmatism and the Geodynamic Evolution of the Northern Taiwan Region. Journal of Petrology 45(5), 975-1011.

Xiang, Y-X., Yang, J-H., Chen J-Y., Zhang, Y. 2017. Petrogenesis of Lingshan highly fractionated granites in the southeast China: Implication for

Nb-Ta mineralization. Ore Geology Review 89, 495-525.

Yılmaz, Y. 1989. An approach to the origin of young volcanic rocks of western Turkey. In: Şengör AMC (eds) Tectonic evolution of the Tethyan Region. Kluwer, Dordrecht, pp. 159.

Yılmaz, Y. 1990. Comparison of the young volcanic associations of the West and the east Anatolia under the compressional regime: a review. Journal of volcanology and geothermal Research 44, 69-87.

Yılmaz, Y. 1997. Geology of western Anatolia. Active tectonics of northwestern Anatolia. The Marmara poly-project, a multidisciplinary approach by space-geodesy, geology, hydrogeology, geothermic and seismology. Vdf Hochschulverlag AG an der Zurich, pp 31–53.

Yılmaz, Y., Tüysüz, O., Gözübol, A.M., Yiğitbaş, E. 1981. Abant (Bolu)-Dokurcan (Sakarya) arasındaki Kuzey Anadolu Fay Zonunun kuzey ve güneyinde kalan tektonik birliklerin jeolojik evrimi: İst. Yerbilimleri 1, 23, 9-261.

Yılmaz, Y., Genç, Ş.C., Yiğitbaş, E., Bozcu, M. Yılmaz, K. 1995. Geological evolution of the Late Mesozoic continental margin of Northwestern Anatolia. Tectonophysics 243, 155-171.

Yılmaz, Y., Genç Ş.C., Karacık, Z., Altunkaynak, Ş. 2001. Two contrasting magmatic associations of NW Anatolia and their tectonic significance. Journal of Geodynamics 31, 243-271.

Yılmaz Şahin, S., Örgün, Y., Güngör, Y., Göker, A.F., Gültekin, A.H., Karacık, Z. 2010. Mineral and Whole-rock Geochemistry of the Kestanbol Granitoid (Ezine-Çanakkale) and its Mafic Microgranular Enclaves in Northwestern Anatolia: evidence of felsic and mafic magma interaction. Turkish Journal of Earth Science 19, 101-122.

Yiğit, Ö. 2012. A prospective sector in the Tethyan Metallogenic Belt: Geology and geochronology of mineral deposits in the Biga Peninsula, NW Turkey. Ore Geology Reviews 46, 118-148.

Appendix 1- Location and description of samples. Abbreviatons: Q: Quartz; plag: plagioclase.

Sample No	Location		Description								
			Sampling	*Petrographical classification*	*Texture*	*Grain size*	*Felsic minerals*	*Mafic minerals*	*Accessory minerals*	*Alteration*	*Others*
Karabiga Gt.											
ASM-K11	40°25'10".69	27°16'4".77	Dike	Granite Aplite	Holocrystalline granular texture	fine	Q, orthoclase, plag	biotite	opaque min., zircon	low sericitization, argillisation	Some orthoclase minerals exhibit graphic texture.
ASM-K12	40°25'50".49	27°11'36".83	Stock	Granite Aplite	Holocrystalline granular texture	fine-medium	Q, orthoclase, plag	biotite	opaque min.	moderate sericitization, argillisation	
ASM-K13	40°25'47".23	27°11'13".48	Dike	Granite-porphyry	Holocyrstalline porphyric texture	medium-coarse	Phenocrysts: Q, orthoclase, plag Groundmass: Q, orthoclase, plag	biotite	opaque min.	low sericitization, argillisation	Some orthoclase minerals exhibit graphic texture.
ASM-K14	40°25'57".76	27°12'13".05									
ASM-K15	40°25'49".56	27°13'6".21									
ASM-K16	40°26'50".84	27°15'7".22									
Güreci Gt.											
ASM-K01	40°21'32".34	26°56'19".59	Stock	Granite	Holocrystalline granular texture	medium	plag, orthoclase, Q	biotite, hornblende	opaque min.	low sericitization, argillisation, chloritisation	Some orthoclase minerals exhibit poikilitic texture.
ASM-K02	40°21'18".11	26°56'38".97	Stock	Granite	Holocrystalline granular texture	medium	plag, orthoclase, Q	biotite, hornblende	sphene (titanite), opaque min.	moderate-high sericitization,argillisation, chloritisation, epidotization	Some orthoclase minerals exhibit poikilitic texture.
ASM-K03	40°21'28".95	26°56'40".19	Stock	Granite	Holocrystalline granular texture	medium	plag, orthoclase, Q	biotite, hornblende	sphene (titanite), opaque min.	low sericitization, argillisation, chloritisation	Some orthoclase minerals exhibit graphic texture.
ASM-K04	40°21'22".14	26°53'3".61									
ASM-K05	40°20'57".90	26°53'28".87									
ASM-K06	40°17'0".84	26°52'9".47	Stock	Monzonite	Holocrystalline granular texture	fine-medium	plag, orthoclase, Q	hornblende	sphene (titanit), opaque min.	moderate sericitization, argillisation	
ASM-K07	40°17'0".27	26°52'21".58	Stock	Q-diorite	Holocrystalline granular texture	medium-coarse	plag, orthoclase, Q	hornblende, biotite	sphene (titanit), opaque min.	low-moderate sericitization, argillisation, chloritisation	Some orthoclase minerals exhibit poikilitic texture. The sample has been subjected to cataclasm and recyrstallisation occurred in Q minerals
ASM-K08	40°17'2".67	26°52'25".89									
ASM-K09	40°17'4".19	26°52'0".10									
ASM-K10	40°17'14".58	26°52'3".56									
Kuşçayır Gt.											
ASM-K48	39°55'39".38	26°36'13".92	Stock	Q-monzodiorite	Holocrystalline porphyric texture	medium-coarse	Q, plag, K-feldspar	hornblende	opaque min.	low argillisation, opacification	Hornblende contains the exsolution lamellae of opaque mineral
ASM-K49	39°55'51".22	26°36'15".29	Stock								

Appendix 1- (Continue)

Sample No	Location			Description							
				Sampling	*Petrographical classification*	*Texture*	*Grain size*	*Felsic minerals*	*Mafic minerals*	*Accessory minerals*	*Alteration*	*Others*
ASM-K50		39°56'5".17	26°36'6".40	Stock	Q-monzodiorite	Holocrystalline porphyric texture	medium-coarse	Q, plag, K-feldspar	hornblende	opaque min.	low argillisation, opacification	Hornblende contains the exsolution lamellae of opaque mineral
ASM-K51		39°56'11".99	26°35'50".06	Stock								
ASM-K52		39°56'13".68	26°35'12".84									
Dikmen Gt.												
ASM-K56		40°8'58".88	27°10'36".98	Stock	Granodiorite	Holocrystalline granular texture	medium	Q, plag, orthoclase	biotite, hornblende	opaque min.	low-moderate sericitization, chloritisation	Plagioclase minerals have biotite inclusions and, fragmention occurs along grain boundary. Hornblende has poikilitic texture and some have plagioclase inclusions. Chloritisation of biotite from the cleavages is observed and some hornblende minerals were transfomed into biotite
ASM-K57		40°8'57".66	27°10'32".37									
ASM-K58		40°8'54".75	27°10'27".58									
Sarıoluk Gt												
ASM-K25		40°7'32".58	27°23'26".72	Stock	Granodiorite	Holocrystalline granular texture	fine-medium	Q, plag, orthoclase	biotite, pyroxene	opaque min.	low-moderate argillitisation, uralitisation	micrographic texture in some orthoclase minerals
ASM-K26		40°7'43".98	27°23'58".85									
ASM-K27		40°8'34".90	27°26'39".11	Stock	Granodiorite	Holocrystalline granular texture	fine-medium	Q, plag, orthoclase	biotite, hornblende	opaque min., sphene (titanite)	low-moderate argillitization, carbonatisation	micrographic texture in some orthoclase minerals
ASM-K28		40°8'43".66	27°27'11".58									
ASM-K29		40°8'49".31	27°28'6".56									
ASM-K30		40°8'48".91	27°28'26".63									
Yenice Gt												
ASM-K31	**Çakuroba**	39°57'13".05	27°17'36".26	Stock	Granite	Holocrystalline granular texture	medium-coarse	plag, orthoclase, Q	biotite, hornblende (pyroxene residue)	opaque min., sphene (titanite)	moderate sericitization, chloritisation	
ASM-K32		39°57'21".68	27°17'20".62									
ASM-K33		39°57'19".96	27°16'44".03									
ASM-K59	**Hamdibey**	39°55' 19".40	27°16'14".13									
ASM-K60		39°53' 59".90		Stock	Granodiorite	Holocrystalline granular texture	medium	Q, plag, orthoclase	biotite, hornblende	sphene (titanite), opaque min.	low-moderate sericitization, chloritisation	Hornblende with a poikilitic texture has plagioclase inclusions. Chloritisation of biotite through cleavages is observed, some hornblendes are transfromed into biotite
ASM-K61		39°51'51".19	27°12'59".33	Stock	Granodiorite	Holocrystalline granular texture	medium	Q, plag, orthoclase	biotite, hornblende	opaque min.	low argillisation	Grain size reduction due to cataclastism
ASM-K62		39°52'19".40	27°13'20".38									
ASM-K63		39°52'49".06	27°12'54".25									

Appendix 1- (Continue)

Sample No	Location			Description								
				Sampling	*Petrographical classification*	*Texture*	*Grain size*	*Felsic minerals*	*Mafic minerals*	*Accessory minerals*	*Alteration*	*Others*
ASM-K53	**Eskiyayla**	39°54'53".61	27°1'22".26	Stock	Granite	Holocrystalline granular texture	fine	Q, microcline, orthoclase, plag.	biotite, hornblende	opaque min.	low sericitization, carbonatisation	sieve texture in plagioclase, perthitic texture in orthoclase
ASM-K54		39°54'33".83	27°1'1".66									
ASM-K55		39°54'10".15	27°1'34".63									
Kestanbol Gt.												
ASM-K41		39°44'45".76	26°18'35".99	Stock	Q-monzonite	Holocrystalline granular texture	fine	Q, plag, K-feldspar	biotite	opaque min.		mafic minerals forms glameroporphyric texture
ASM-K42		39°43'28".16	26°17'44".59									
ASM-K43		39°42'53".64	26°17'0".97	Stock	Granite	Holocrystalline granular texture	medium-coarse	Q, plag, K-feldspar	biotite, hornblende	sphene (titanite), opaque min.		poikilitic and perthitic texture in K-feldspars
ASM-K44		39°42'38".41	26°15'55".74									
ASM-K45		39°42'54".89	26°15'6".05									
ASM-K46		39°46'24".24	26°16'3".48	Dike	Lamprophyre/ Kersantite	Porphyric texture	fine	Plag, K-feldspar	pyroxene, biotite, olivine (?)	opaque min.	low argillisation	
ASM-K47		39°46'24".24	26°16'3".48	Dike								
Eybek Gt.												
ASM-K64		39°42'39".60	27°10'18".18	Stock	Q-monzonite	Holocrystalline granular texture	fine	plag, orthoclase, Q	biotite, hornblende	sphene (titanite), opaque min., zircon	low sericitization, chloritisation, opasitleşme	Orthoclase minerals exhibit poiklitic texture, and contains plagioclase and hornblende inclusions. Hornblende contains the exsolution lamellae of opaque mineral and exhibit chloritisation and some are also transformed into biotite
ASM-K65		39°42'30".52	27°9'55".90	Stock	Granite	Holocrystalline granular texture	medium	Q, orthoclase, plag	biotite, hornblende	sphene (titanite), opaque min.	low-moderate sericitization, opasitleşme	Orthoclase minerals exhibit poikilitic texture. Hornblende contains the exsolution lamellae of opaque mineral.
ASM-K66		39°41'11".92	27°9'39".01	Stock	Granodiorite	Holocrystalline granular texture	medium	Q, plag, orthoclase	biotite	sphene (titanite), opaque min.	low argillitization	
ASM-K67		39°40'53".68	27°9'20".45									
ASM-K69		39°40'53".58	27°9'9".07									
ASM-K70		39°41'10".94	27°8'30".36									
Evciler Gt												
ASM-K34		39°46'36".54	26°41'32".06	Stock	Granodiorite	Holocrystalline granular texture	medium	Q, plag, orthoclase	biotite, hornblende	sphene (titanite), opaque min.	moderate sericitization, argillitization, chloritisation	poikilitic texture in some orthoclase minerals

Appendix 1- (Continue)

Sample No	Location		Description								
			Sampling	*Petrographical classification*	*Texture*	*Grain size*	*Felsic minerals*	*Mafic minerals*	*Accessory minerals*	*Alteration*	*Others*
ASM-K35	39°47'5".71	26°42'24".94	Stock	Granodiorite	Holocrystalline granular texture	medium-coarse	Q, K-feldspar, plag	biotite, hornblende	sphene (titanite), opaque min.	low chloritisation, sericitization	Myrmekitic texture developed between quartz and plagioclase.Chloritisation of biotite and hornblende through the cleavages is observed. Q minerals have plagioclase inclusions.
ASM-K36	39°47'41".25	26°45'41".61			Holocrystalline granular texture	medium					
ASM-K37	39°48' 3".02	26°46'49".15	Stock	Granite Aplite	Holocrystalline granular texture		Q, K-feldspar, plag	rare biotite	opaque min.	low argillisation, sericitization	Perthitic and graphic texture
ASM-K38	39°48'35".70	26°47'18".57									
ASM-K39	39°48'35".70	26°47'18".57									
ASM-K40	39°50'22".06	26°54'12".47									
Camyayla Gt											
ASM-K20	40°6'37".02	26°44'57".02									
ASM-K21	40°6'30".98	26°44'39".98	Stock	Q-monzodiorite porphyry	Holocyrstalline porphyric texture	medium-coarse	Phenocrysts: plag Groundmass: plag, orthoclase, Q	Groundmass: biotite, hornblende	opaque min.	Orta sericitization, argillisation, chloritisation	Some orthoclase minerals exhibit micrographic texture.
ASM-K22	40°6'42".23	26°44'23".59	Stock								
ASM-K23	40°7'2".05	26°44'12".24	Stock	Q-monzodiorite	Holocrystalline granular texture	fine-medium	plag, orthoclase, Q	biotite, hornblende	opaque min.	low-moderate sericitization, argillisation, chloritisation	Some orthoclase minerals exhibit micrographic texture.
ASM-K24	40°7'14".47	26°44'51".73	Stock								
Alanköy Gt											
ASM-K17	40°1'18".71	26°46'32".43	Stock	Q-diorite	Holocrystalline granular texture	medium	plag, Q, orthoclase	hornblende	sphene (titanite), opaque min.	high sericitization, argillisation, chloritisation, epidotization	
ASM-K18	40°1'12".34	26°46'41".86									
ASM-K19	40°1'18".55	26°46'31".72	Stock								